Aberrant regulation of the GSK-3β/NRF2 axis unveils a novel therapy for adrenoleukodystrophy

Pablo Ranea-Robles, Nathalie Launay, Montserrat Ruiz, Noel Ylagan Calingasan, Magali M Dumont, Alba Naudí, Manuel Portero-Otín, Reinald Pamplona, Isidre Ferrer, M Flint Beal, et al.

HAL Id: hal-02120916

https://hal.sorbonne-universite.fr/hal-02120916v1

Submitted on 6 May 2019

SOURCE
DATA

TRANSPARENT
PROCESS

OPEN
ACCESS

EMBO
Molecular Medicine

Research Article

Aberrant regulation of the GSK-3β/NRF2 axis unveils a novel therapy for adrenoleukodystrophy

Pablo Ranea-Robles[1,2] (iD), Nathalie Launay[1,2], Montserrat Ruiz[1,2], Noel Ylagan Calingasan[3], Magali Dumont[4], Alba Naudí[5], Manuel Portero-Otín[5], Reinald Pamplona[5], Isidre Ferrer[6,7,8,9], M Flint Beal[3], Stéphane Fourcade[1,2,*] (iD) & Aurora Pujol[1,2,10,**] (iD)

Abstract

The nuclear factor erythroid 2-like 2 (NRF2) is the master regulator of endogenous antioxidant responses. Oxidative damage is a shared and early-appearing feature in X-linked adrenoleukodystrophy (X-ALD) patients and the mouse model (*Abcd1* null mouse). This rare neurometabolic disease is caused by the loss of function of the peroxisomal transporter ABCD1, leading to an accumulation of very long-chain fatty acids and the induction of reactive oxygen species of mitochondrial origin. Here, we identify an impaired NRF2 response caused by aberrant activity of GSK-3β. We find that GSK-3β inhibitors can significantly reactivate the blunted NRF2 response in patients' fibroblasts. In the mouse models (*Abcd1⁻* and *Abcd1⁻/Abcd2⁻/⁻* mice), oral administration of dimethyl fumarate (DMF/BG12/Tecfidera), an NRF2 activator in use for multiple sclerosis, normalized (i) mitochondrial depletion, (ii) bioenergetic failure, (iii) oxidative damage, and (iv) inflammation, highlighting an intricate cross-talk governing energetic and redox homeostasis in X-ALD. Importantly, DMF halted axonal degeneration and locomotor disability suggesting that therapies activating NRF2 hold therapeutic potential for X-ALD and other axonopathies with impaired GSK-3β/NRF2 axis.

Introduction

Oxidative stress and mitochondrial dysfunction contribute to the onset and progression of age-related neurodegenerative diseases, such as amyotrophic lateral sclerosis, Parkinson's, Huntington's, and Alzheimer's disease (Lin & Beal, 2006). A common theme among these disorders, as well as the prototypic demyelinating disease multiple sclerosis, is axonal degeneration (Li *et al*, 2001; Tallantyre *et al*, 2010).

Endogenous antioxidant responses are controlled by nuclear factor erythroid 2-like 2 (NRF2, encoded by *NFE2L2*), which binds to antioxidant response element (ARE) in the promoter region of target genes, subsequently activating the transcription of genes encoding phase II detoxifying enzymes and cytoprotective defences against oxidative stress (Itoh *et al*, 1997). These genes include heme oxygenase-1 (*HMOX1*), NAD(P)H:quinone oxidoreductase-1 (*NQO1*), and enzymes of glutathione metabolism, such as glutathione S-transferases (*GST*), glutamate-cysteine ligase (*GCL*), and glutathione peroxidases (McMahon *et al*, 2001; Lee *et al*, 2003). NRF2 also regulates proteostasis (Komatsu *et al*, 2010; Pajares *et al*, 2016), neuroinflammation (Innamorato *et al*, 2008; Rojo *et al*, 2010), and bioenergetic homeostasis (Holmstrom *et al*, 2013) in the nervous system, such that activating NRF2-dependent responses initiates a sustained neuroprotective effect in several neurodegenerative disorder models (Kanninen *et al*, 2009; Neymotin *et al*, 2011; Stack *et al*, 2011; Kaidery *et al*, 2013; Lastres-Becker *et al*, 2016). We therefore sought to explore the role of NRF2 pathway in the neurodegenerative processes of X-linked adrenoleukodystrophy (X-ALD; McKusick no. 300100).

This is the most common peroxisomal disease and leukodystrophy with an incidence of 1:15,000 (Kemper *et al*, 2017). It is caused by mutations in the *ABCD1* gene (Mosser *et al*, 1993) located on

Xq.28, which encodes a peroxisomal transporter that moves very long-chain fatty acids (VCLFA) into the peroxisome for degradation by β-oxidation (van Roermund *et al*, 2008; Wiesinger *et al*, 2013). As a consequence, very long-chain fatty acids (VLCFA), especially C26:0, accumulate in tissues and plasma and constitute a pathognomonic biomarker for diagnosis. There are two main forms of the disease (Engelen *et al*, 2012). First, cerebral adrenoleukodystrophy is present mostly in boys between 5 and 10 years (35–40% of the cases) but also in adolescents and adult men, who present a strong inflammatory demyelinating reaction in central nervous system white matter. Second, adrenomyeloneuropathy occurs in 60% of the cases and affects adult men and heterozygous women over the age of 40 (Engelen *et al*, 2014). Adrenomyeloneuropathy is characterized by peripheral neuropathy and distal axonopathy involving corticospinal tracts of the spinal cord. The clinical presentation of X-ALD varies even in the same family, which suggests the presence of modifier genes or environmental factors (Berger *et al*, 1994; Turk *et al*, 2017). Current therapeutic options are restricted to bone marrow transplantation (Miller *et al*, 2011) and hematopoietic stem cell gene therapy (Cartier *et al*, 2009; Eichler *et al*, 2017), and are limited by a very narrow therapeutic window, which reinforces the need to develop additional therapies for this devastating disease.

The mouse model of X-ALD (*Abcd1⁻* mice) develops axonopathy and locomotor impairment very late in life, at 20 months of age, resembling adrenomyeloneuropathy, the most frequent X-ALD phenotype (Pujol *et al*, 2002). The closest homolog *Abcd2* exhibits overlapping metabolic functions (Fourcade *et al*, 2009) and has been postulated as modifier of the biochemical defect (Muneer *et al*, 2014). Double mutant *Abcd1⁻/Abcd2⁻/⁻* mice develop a more severe, earlier onset axonopathy starting at 12 months of age, what makes them a more suitable model for therapeutic essays (Pujol *et al*, 2002; Mastroeni *et al*, 2009; Lopez-Erauskin *et al*, 2011; Morato *et al*, 2013, 2015; Launay *et al*, 2015, 2017). Using these mouse models and patients' samples, studies by our laboratory and others have revealed that VLCFA-induced oxidative stress is a critical, early pathogenic factor in X-ALD (Vargas *et al*, 2004; Powers *et al*, 2005; Fourcade *et al*, 2008, 2010; Hein *et al*, 2008; Lopez-Erauskin *et al*, 2011; Petrillo *et al*, 2013), although the exact mechanisms by which VLCFA-induced redox imbalance causes neurodegeneration in X-ALD remain unclear (Fourcade *et al*, 2015). Here, we examined whether the NRF2 antioxidant pathway could contribute to the increased oxidative damage detected in this disease, in both the *Abcd1⁻* mouse model and the skin fibroblasts derived from X-ALD patients. We also treated X-ALD mouse models (*Abcd1⁻* and *Abcd1⁻/Abcd2⁻/⁻* mice) with dimethyl fumarate (DMF, BG-12, Tecfidera), an NRF2 activator (Linker *et al*, 2011; Scannevin *et al*, 2012), that is a currently approved medication for relapsing-remitting multiple sclerosis (Fox *et al*, 2012; Gold *et al*, 2012).

Results

GSK-3β/NRF2 antioxidant pathway is altered in *Abcd1⁻* mice

We previously identified a redox dyshomeostasis in X-ALD, characterized by an excess of reactive oxygen species (ROS) production and repression of key antioxidant enzymes (Fourcade *et al*, 2008). Since NRF2 plays a critical role in the antioxidant cellular defence,

we asked whether the NRF2-dependent antioxidant pathway was altered in the *Abcd1* null mouse. We found decreased NRF2 protein levels in *Abcd1⁻* mice spinal cord at 12 months of age (Fig 1A), a presymptomatic disease stage in this mouse model. Dysregulated NRF2 protein levels were organ-specific, as we did not observe any changes in non-affected tissues in the mouse model, such as cerebral cortex or liver (Fig EV1). To verify that lower protein levels had functional consequences, we measured mRNA expression of NRF2 classical target genes (*Hmox1*, *Nqo1* and glutathione S-transferase alpha-3, *Gsta3*) at the same age. We observed a slight but significant decreased expression of these three NRF2 target genes in the *Abcd1⁻* mouse spinal cord at 12 months of age (Fig 1B), consistent with a downregulated NRF2 pathway.

Several signals can regulate NRF2-dependent responses, in particular those that modulate GSK-3β activity (Salazar *et al*, 2006; Rojo *et al*, 2008; Rada *et al*, 2011). We thus examined the activity of the AKT/GSK-3β pathway in the spinal cord of *Abcd1⁻* mice by measuring the phosphorylation of serine 473 (pSer473) and threonine 308 (pThr308) residues of AKT, which reflects its activation. We also measured the phosphorylation of serine 9 (pSer9) and tyrosine 216 (pTyr216) residues of GSK-3β, which indicate inhibition or activation of GSK-3β, respectively. We found less AKT activation in *Abcd1⁻* mice spinal cord, as shown by decreased pThr308 AKT relative to total AKT levels. Defective AKT phosphorylation resulted in the activation of GSK-3β, indicated by reduced pSer9 GSK-3β compared with total GSK-3β levels (Fig 1C and D). We did not observe any changes in pSer473, pTyr216, or in the total levels of AKT and GSK-3β (Fig 1C and D). These data indicate a dysregulated AKT/GSK-3β/NRF2 axis in the *Abcd1⁻* mouse spinal cord, with predicted higher activity of GSK-3β upstream of NRF2.

Impaired NRF2-dependent antioxidant pathway is mediated by GSK-3β in patients' fibroblasts

Primary fibroblasts from X-ALD patients provide a good surrogate cell model to dissect disease mechanisms, as they recapitulate the main disease hallmarks: accumulation of VLCFA (Moser *et al*, 1980), higher production of free radicals of mitochondrial origin (Lopez-Erauskin *et al*, 2013), loss of energetic homeostasis (Galino *et al*, 2011), altered proteostasis (Launay *et al*, 2013, 2015), and endoplasmic reticulum (ER) stress (van de Beek *et al*, 2017; Launay *et al*, 2017). Using this cell system, we determined whether patients' fibroblasts exhibited an altered AKT/GSK-3β/NRF2 pathway.

At baseline, we observed equivalent NRF2 protein levels in patients' fibroblasts compared with controls (Fig EV1).

We then tested the functionality of the NRF2 pathway, by treating patients' and control fibroblasts either with C26:0, the primary VLCFA accumulated in patients, or with oligomycin, which acts as a generator of mitochondrial ROS inhibiting complex V (Fourcade *et al*, 2008; Paupe *et al*, 2009). Both compounds produce mitochondrial ROS in these fibroblasts (Lopez-Erauskin *et al*, 2013). We show that both C26:0 and oligomycin activated NRF2-dependent responses in control fibroblasts, characterized by both higher NRF2 translocation to the nucleus (Fig 2A and B) and increased expression of NRF2 target genes (*HMOX1*, *NQO1,* and *GCLC* mRNA; Fig 2C). However, this physiological response against oxidative stress was blunted in X-ALD fibroblasts with both ROS-producing stimuli (Fig 2A–C).
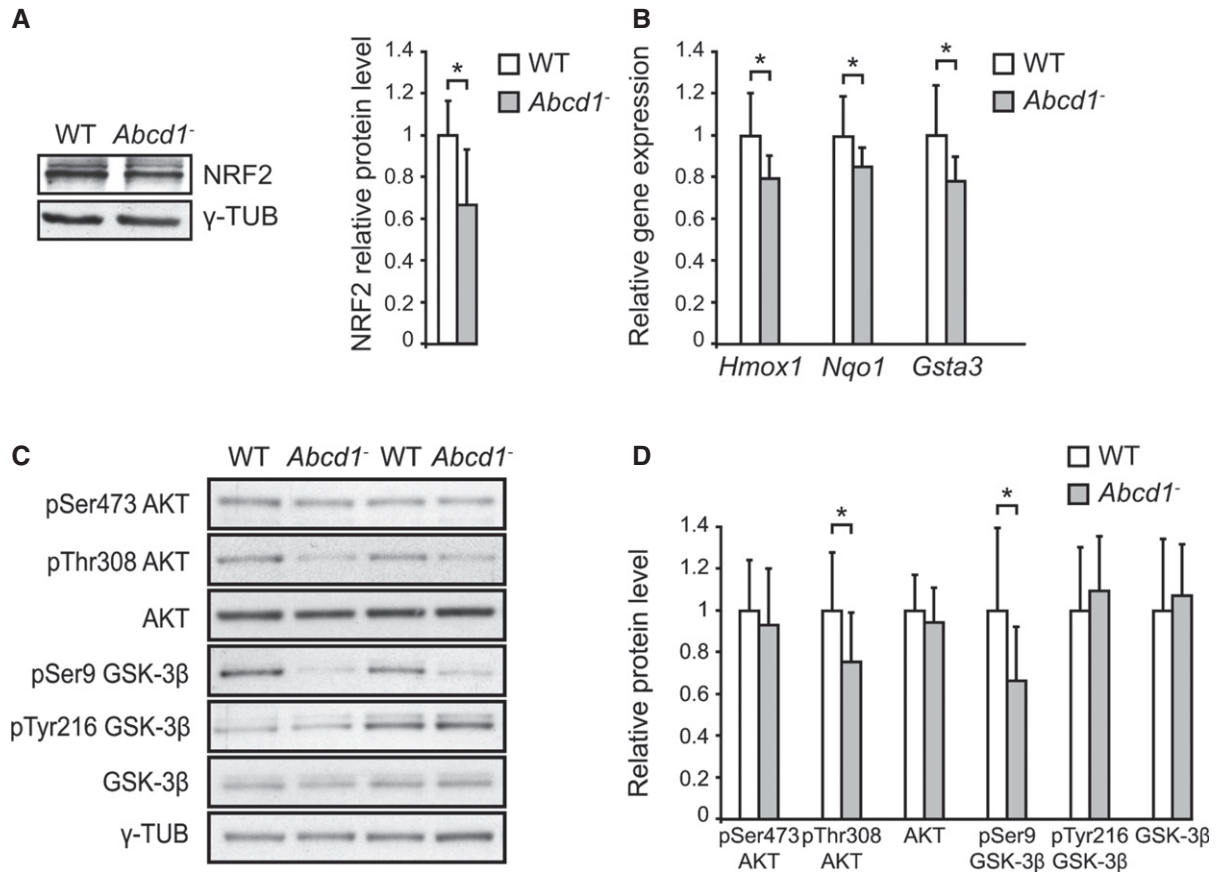
Figure 1.   Altered GSK-3β/NRF2 antioxidant pathway in *Abcd1⁻* mice.

A   Representative immunoblot of NRF2 protein level measured in WT (*n* = 6) and *Abcd1⁻* (*n* = 6) mice spinal cord at 12 months of age. Protein levels normalized relative to γ-tubulin (γ-TUB) and quantification depicted as fold change to WT mice.

B   NRF2-dependent antioxidant gene expression (*Hmox1, Nqo1,* and *Gsta3*) in WT (*n* = 8) and *Abcd1⁻* (*n* = 8) mice spinal cord at 12 months of age. Gene expression normalized relative to mouse *Rplp0* and depicted as fold change to WT mice.

C, D   Representative immunoblots of pSer473 AKT, pThr308 AKT, AKT, pSer9 GSK-3β, pTyr216 GSK-3β, and GSK-3β protein level in WT (*n* = 12) and *Abcd1⁻* (*n* = 12) mice spinal cord at 12 months of age. Protein level normalized relative to corresponding non-phosphorylated proteins or γ-TUB (in the case of AKT and GSK-3β). Quantification depicted as fold change to WT mice.

Data information: In (A, B, and D), data are presented as mean ± SD. *$P < 0.05$ (unpaired Student's *t*-test). See the exact *P*-values in Appendix Table S3.

Source data are available online for this figure.

Moreover, both treatments elicited AKT activation (increased pSer473 and pThr308) and subsequent GSK-3β inactivation (higher pSer9 GSK-3β levels) in control fibroblasts (Fig 2D and E). Again, this physiological response against oxidative stress was impaired in X-ALD fibroblasts, as phosphorylated levels of AKT and GSK-3β did not change following C26:0 or oligomycin treatment (Fig 2D and E).

As GSK-3β activation can repress NRF2, we sought to determine whether this phenomenon was interrelated in the cellular model. For this, we assessed whether specific GSK-3β inhibitors (CT99021 and SB216763; Coghlan *et al*, 2000; Ring *et al*, 2003) could restore a normal NRF2-dependent response in X-ALD fibroblasts. Indeed, treatment with both compounds reactivated the NRF2 pathway, characterized by an upregulation of the NRF2-target genes *HMOX1, NQO1,* and *GCLC* in patients' fibroblasts upon incubation with excess of C26:0 (Fig 2F).

Collectively, these data indicate that the aberrant GSK-3β activation upstream of NRF2 governs the blunted NRF2-dependent response upon oxidative stress in this disease model.

DMF rescues mitochondrial depletion, bioenergetic failure, and oxidative damage in *Abcd1⁻* mice

To elucidate the impact of a defective NRF2-dependent response in the pathogenesis of adrenoleukodystrophy, we decided to treat *Abcd1⁻* mice with DMF, a classical activator of NRF2 (Linker *et al*, 2011; Scannevin *et al*, 2012). Dimethyl fumarate has therapeutic efficacy for relapsing-remitting multiple sclerosis (Fox *et al*, 2012; Gold *et al*, 2012) and besides, preclinical tests show success to treat other neurodegenerative diseases like Huntington's (Ellrichmann *et al*, 2011) and Parkinson's disease (Ahuja *et al*, 2016; Lastres-Becker *et al*, 2016).

Before treating the animals, we tested DMF in control and X-ALD fibroblasts. We found that DMF reactivated the NRF2-blunted response upon VLCFA addition (Fig EV2), similar to the GSK-3β inhibitors used (Fig 2F). Moreover, DMF alone induced *HMOX1* and *NQO1* expression in control fibroblasts and also *HMOX1* expression

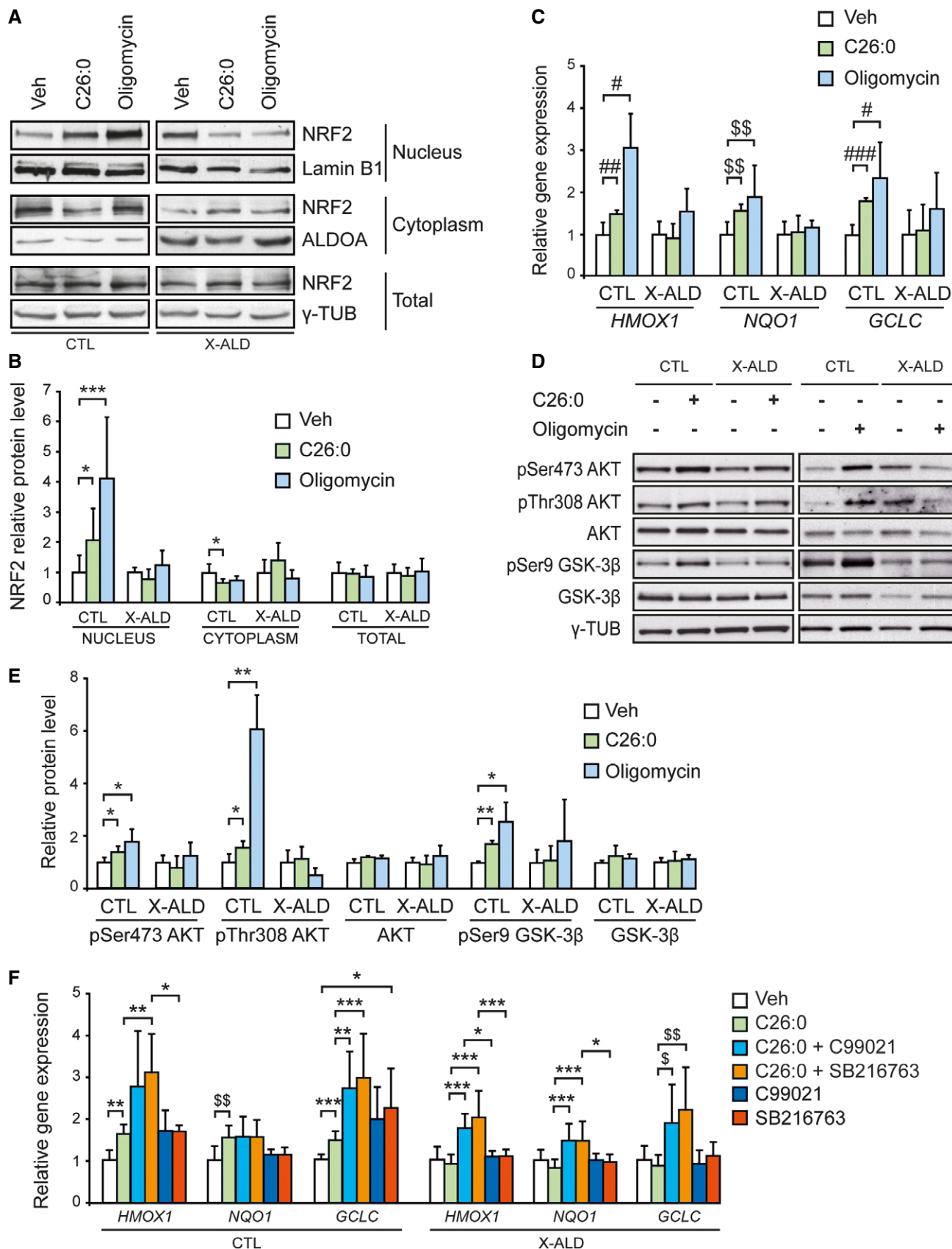**Figure 2.**

◄

Figure 2.   Impaired AKT/GSK-3β/NRF2 antioxidant response after oxidative stress in X-ALD patients' fibroblasts.

A, B   Representative immunoblots of NRF2 protein translocation to the nucleus upon VLCFA (C26:0, 50 μM, 24 h) or oligomycin (15 μM, 18 h) in control (CTL, *n* = 5 per condition, left panels) and X-ALD (*n* = 5 per condition, right panels) fibroblasts. Protein levels normalized relative to lamin B1 in the nuclear fraction, aldolase A (ALDOA) in the cytoplasmic fraction, and γ-TUB in the total fraction. Quantification depicted as fold change to vehicle-treated (Veh) fibroblasts.

C   NRF2-dependent antioxidant gene expression (*HMOX1, NQO1,* and *GCLC*) upon oxidative stress in CTL (*n* = 5 per condition) and X-ALD (*n* = 5 per condition) fibroblasts. Gene expression normalized relative to *RPLP0*. Quantification depicted as fold change to vehicle-treated (Veh) fibroblasts.

D, E   Representative immunoblots of pSer473 AKT, pThr308 AKT, AKT, pSer9 GSK-3β, and GSK-3β measured after oxidative stress in CTL (*n* = 5 per condition) and X-ALD (*n* = 5 per condition) fibroblasts. Protein levels normalized relative to corresponding non-phosphorylated proteins or γ-TUB (in the case of AKT and GSK-3β). Quantification depicted as fold change to vehicle-treated (Veh) fibroblasts.

F   NRF2-dependent antioxidant gene expression (*HMOX1, NQO1,* and *GCLC*) after GSK-3β inhibition in VLCFA-treated CTL (*n* = 8 per condition) and X-ALD (*n* = 8 per condition) fibroblasts. Gene expression normalized relative to *RPLP0*. Quantification depicted as fold change to vehicle-treated (Veh) fibroblasts.

Data information: In (B, C, E, and F), data are presented as mean ± SD. In (B, E, and F), *$*P < 0.05$, $**P < 0.01$, $***P < 0.001$ (one-way ANOVA followed by Tukey's *post hoc* test). In (C), $^{\#}P < 0.05$, $^{\#\#}P < 0.01$, $^{\#\#\#}P < 0.001$ (one-way ANOVA followed by Dunnett's *post hoc* test). In (C and F), $^{\$}P < 0.01$, $^{\$\$}P < 0.01$ (non-parametric Kruskal–Wallis' test followed by Dunn's *post hoc* test). See the exact *P*-values in Appendix Table S3.
Source data are available online for this figure.

in X-ALD fibroblasts (Fig EV2). Thus, these new data reinforced the rational for DMF treatment *in vivo*.

We fed *Abcd1⁻* mice with DMF-containing chow at 100 mg/kg, starting at 8 months of age, for 4 months. First, we verified the efficacy of dietary DMF administration by measuring NRF2 protein levels and mRNA expression of three classical NRF2-target genes (*Hmox1, Nqo1,* and *Gsta3*). Dimethyl fumarate treatment rescued both NRF2 protein levels (Fig 3A) and NRF2 targets in *Abcd1⁻* mice spinal cord at 12 months of age (Fig 3B).

Next, we measured the effect of DMF on several quantitative markers of oxidative damage to lipids and proteins, such as direct carbonylation of proteins (Aminoadipic semialdehyde: AASA), glycoxidation (Nε-(carboxyethyl)-lysine: CEL and Nε-(carboxy-methyl)-lysine: CML), and protein lipoxidation (Nε-malondialde-hyde-lysine: MDAL; Fourcade *et al*, 2008). We found an antioxidant role for DMF in this model, as it normalized AASA, CEL, CML, and MDAL in *Abcd1⁻* mice spinal cord (Fig 3C).

We also examined the effect of DMF on mitochondrial dysfunction (Morato *et al*, 2013, 2015). DMF normalized mitochondrial biogenesis, based on different parameters: mtDNA levels (Fig 3D) and mRNA expression of sirtuin-1, *Sirt1*; peroxisome proliferator-activated receptor gamma coactivator 1-alpha, *Ppargc1a*; nuclear respiratory factor-1, *Nrf1*; and transcription factor A, mitochondrial, *Tfam* (Fig 3E; Morato *et al*, 2013, 2015). We previously reported decreased levels of ATP in the spinal cord of *Abcd1⁻* mice (Galino *et al*, 2011), suggesting that deficient energy homeostasis is a key feature in X-ALD pathology. In this study, we reveal that DMF prevented bioenergetic failure, as it normalized ATP levels (Fig 3F). These effects seem to be independent of VLCFA levels, since DMF treatment did not alter C24:0 or C26:0 levels in the spinal cord of 12-month-old *Abcd1⁻* mice (Fig EV3). Altogether, DMF activated NRF2-dependent antioxidant pathway and prevented mitochondrial depletion, bioenergetic failure, and oxidative damage in the spinal cord of the disease mouse model.

DMF treatment prevents inflammatory imbalance in *Abcd1⁻* mice

Although patients presenting with pure adrenomyeloneuropathy do not exhibit overt brain inflammation that induces demyelination, we previously found low-grade inflammatory dysregulation in the *Abcd1⁻* mouse spinal cord and in adrenomyeloneuropathy patients. Our functional genomics assay detected activation of the NF-κB-mediated inflammatory pathway and increased expression of

several pro-inflammatory cytokines in the *Abcd1⁻* mouse spinal cord (Schluter *et al*, 2012). In adrenomyeloneuropathy patients, we recently reported a general dysregulation of inflammatory pathways in peripheral blood mononuclear cells (PBMC) and plasma (Ruiz *et al*, 2015).

Since DMF is also a classical immunomodulatory drug (Schilling *et al*, 2006; Linker *et al*, 2011), we examined its effects on mRNA expression of several inflammation-related genes in the *Abcd1⁻* mice spinal cord. At 12 months of age, *Abcd1⁻* mice exhibited a general imbalance of both pro- and anti-inflammatory markers, characterized by the induction of pro-inflammatory markers including nuclear factor kappa B subunit 2 (*Nfkb2*), interleukin 1 beta (*Il1b*), tumor necrosis factor alpha (*Tnfa*), tumor necrosis factor receptor superfamily member 1a (*Tnfrsf1a*), chemokine (C-C motif) ligand 5 (*Ccl5*), chemokine (C-X-C motif) ligand 9 (*Cxcl9*), chemokine (C-X-C motif) ligand 10 (*Cxcl10*), and chemokine (C-C motif) receptor type 6 (*Ccr6*) (Fig 4A). Also, we observed an upregulation of some anti-inflammatory markers, such as chitinase-like 3 (*Chil3*), chemokine (C-X-C motif) ligand 12 (*Cxcl12*), insulin-like growth factor 1 (*Igf1*), and transforming growth factor, beta 1 (*Tgfb1*) (Fig 4B). Interleukin 6 (*Il6*), resistin like alpha (*Retnla*, also called *Fizz1*), and macrophage migration inhibitory factor (*Mif*) were decreased in the *Abcd1⁻* mouse spinal cord (Fig 4A and B).

Dimethyl fumarate prevented most alterations observed in the inflammatory profile in the *Abcd1⁻* mice spinal cord and normalized mRNA levels of *Nfkb2, Il6, Tnfa, Ccl5, Cxcl10, Ccr6* (pro-inflammatory; Fig 4A), and *Mif, Cxcl12, Tgfb1, Igf1* (anti-inflammatory; Fig 4B). However, DMF had no effect on *Tnfrsf1a, Cxcl9* (pro-inflammatory), and *Fizz1* (anti-inflammatory) mRNA expression in the *Abcd1⁻* mice spinal cord (Fig 4A and B). DMF exacerbated the induction of *Il1b* (pro-inflammatory) and *Chil3* (anti-inflammatory), and induced the expression of interleukin 10 (*Il10*), an anti-inflammatory cytokine, in the *Abcd1⁻* mouse spinal cord (Fig 4A and B). These data demonstrate that DMF normalized the inflammatory profile in *Abcd1⁻* mice.

DMF halts axonal degeneration in *Abcd1⁻/Abcd2⁻/⁻* mice

We then evaluated the effects of DMF on axonal degeneration and locomotor impairment in X-ALD mouse model. We fed *Abcd1⁻/Abcd2⁻/⁻* (DKO) mice with DMF for 6 months, starting at 12 months of age. First, we characterized the immunohistochemical signs of neuropathology present in DKO mice at 18 months of age,
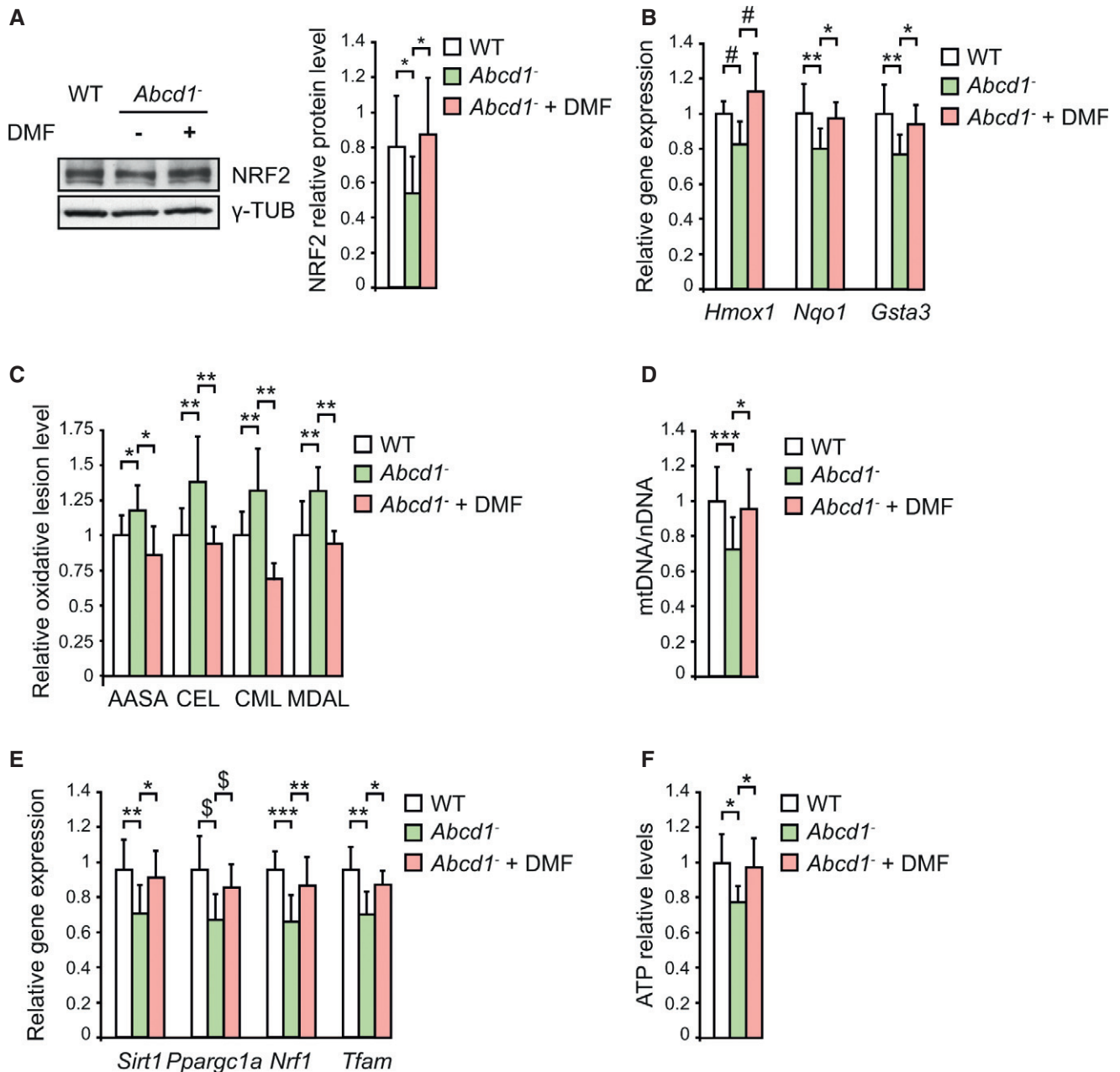
Figure 3. NRF2 activation by DMF prevents oxidative damage to proteins and lipids, mitochondrial depletion, and bioenergetic failure in *Abcd1⁻* mice.

A   Representative immunoblot of NRF2 protein levels in WT ($n = 6$), *Abcd1⁻* ($n = 6$) and DMF-treated *Abcd1⁻* mice (*Abcd1⁻* + DMF, $n = 6$) mice spinal cord at 12 months of age. Protein levels normalized relative to γ-TUB. Quantification depicted as fold change to WT mice.

B   NRF2-dependent antioxidant gene expression (*Hmox1, Nqo1,* and *Gsta3*) in WT ($n = 8$), *Abcd1⁻* ($n = 8$), and *Abcd1⁻* + DMF ($n = 8$) mice spinal cord at 12 months of age. Gene expression normalized relative to *Rplp0*. Quantification represented as fold change to WT mice.

C   Oxidative lesions to lipids and proteins in WT ($n = 5$), *Abcd1⁻* ($n = 5$), and *Abcd1⁻* + DMF ($n = 5$) mice spinal cord at 12 months of age. AASA, CEL, CML, and MDAL levels measured by GC/MS. Quantification represented as fold change to WT mice.

D   mtDNA levels in WT ($n = 8$), *Abcd1⁻* ($n = 8$), and *Abcd1⁻* + DMF ($n = 8$) mice spinal cord at 12 months of age. mtDNA content expressed as the ratio of mtDNA (*CytB* levels) to nDNA (*Cebpa* levels). Quantification depicted as fold change to WT mice.

E   *Sirt1, Ppargc1a, Nrf1,* and *Tfam* gene expression in WT ($n = 8$), *Abcd1⁻* ($n = 8$), and *Abcd1⁻* + DMF ($n = 8$) mice spinal cord at 12 months of age. Gene expression normalized relative to *Rplp0*. Quantification depicted as fold change to WT mice.

F   ATP levels in WT ($n = 8$), *Abcd1⁻* ($n = 8$), and *Abcd1⁻* + DMF ($n = 8$) mice spinal cord at 12 months of age. Quantification represented as fold change to WT mice.

Data information: Data are presented as mean ± SD. *$P < 0.05$, **$P < 0.01$, ***$P < 0.001$ (one-way ANOVA followed by Tukey's *post hoc* test). In (B), [#]$P < 0.05$ (one-way ANOVA followed by Dunnett's *post hoc* test). In (E), [$]$P < 0.05$ (non-parametric Kruskal–Wallis' test followed by Dunn's *post hoc* test). See the exact *P*-values in Appendix Table S3.

Source data are available online for this figure.
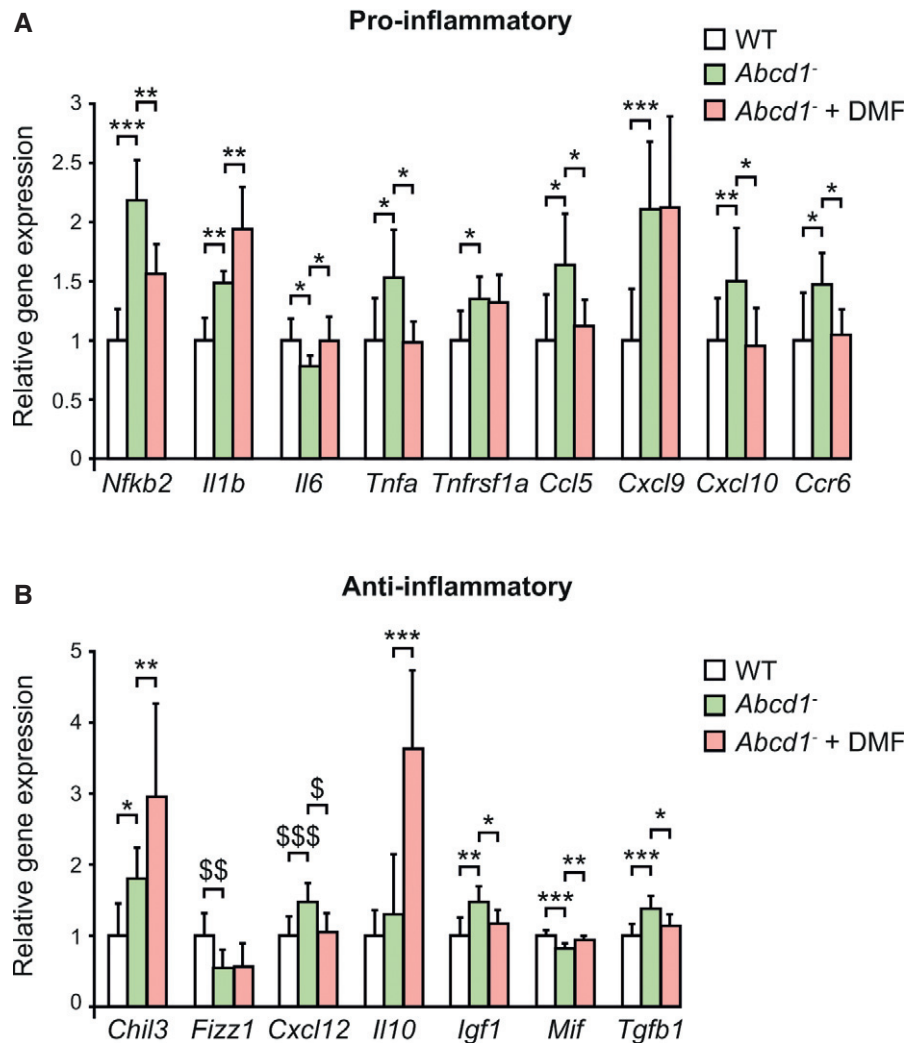
Figure 4. DMF treatment restores inflammatory profile in *Abcd1⁻* mice.

A   Pro-inflammatory (*Nfkb2, Il1b, Il6, Tnfa, Tnfrsf1a, Ccl5, Cxcl9, Cxcl10, Ccr6*) gene expression profile.

B   Anti-inflammatory (*Fizz1, Chil3, Cxcl12, Il10, Igf1, Mif, Tgfb1*) gene expression profile.

Data information: Gene expression was measured in WT (*n* = 8), *Abcd1⁻* (*n* = 8), and *Abcd1⁻* + DMF (*n* = 8) mice spinal cord at 12 months of age. Expression of cytokines, chemokines, and other inflammation-related genes was normalized relative to *Rplp0*. Quantification depicted as fold change to WT mice. Data are presented as mean ± SD. In (A and B), *P < 0.05, **P < 0.01, ***P < 0.001 (one-way ANOVA followed by Tukey's *post hoc* test). In (B), $^{\$}P$ < 0.05, $^{\$\$}P$ < 0.01, $^{\$\$\$}P$ < 0.001 (non-parametric Kruskal–Wallis' test followed by Dunn's *post hoc* test). See the exact *P*-values in Appendix Table S3.

after DMF treatment. We assessed (i) microgliosis; (ii) astrocytosis; (iii) axonal degeneration, shown by accumulation of amyloid precursor protein (APP) and synaptophysin in axonal swellings; (iv) lipidic myelin debris, shown by Sudan Black staining (Pujol *et al*, 2004); (v) oxidative damage to DNA, indicated by increased 8-oxo-7,8-dihydro-2′-deoxyguanosine (8-oxo-dG) staining (Lopez-Erauskin *et al*, 2011); (vi) unhealthy motor neurons with reduced staining of SMI-32, an antibody that labels a non-phosphorylated epitope of neurofilament proteins; and (vii) decreased mitochondrial content observed by cytochrome c (Cyt C) staining in motor neurons (Morato *et al*, 2013; Fig 5A–Y). Dimethyl fumarate reversed microgliosis and astrocytosis, as it normalized the density of astrocytes and microglial cells in DKO mice (Fig 5A–F and Y), prevented axonal accumulation of APP and synaptophysin (Fig 5G–L and Y), halted the appearance of myelin debris along the spinal cord

(Fig 5M–O), and reduced DNA oxidative damage shown by 8-oxo-dG staining (Fig 5P–R) in DKO mice. In addition, motor neuron health and mitochondrial levels improved with DMF treatment (Fig 5S–X). Altogether, these data reveal that DMF treatment significantly ameliorated the neuropathology in *Abcd1⁻/Abcd2⁻/⁻* mice.

DMF reverses locomotor deficits in *Abcd1⁻/Abcd2⁻/⁻* mice

Next, we measured the effect of DMF on the locomotor phenotype of DKO mice using bar cross and treadmill tests at the end of the treatment. As previously described (Pujol *et al*, 2004; Lopez-Erauskin *et al*, 2011), DKO mice at 18 months of age took longer time to cross the bar and slipped off more times while crossing the bar. However, DMF-treated DKO mice behaved similar to wild-type (WT) mice. These data indicate that DMF improved the ability of DKO mice to cross the bar

Figure 5. DMF treatment halts axonal degeneration and locomotor impairment in *Abcd1⁻/Abcd2⁻/⁻* mice.

A–X   Immunohistological analysis of axonal pathologies performed in 18-month-old WT, *Abcd1⁻/Abcd2⁻/⁻* (DKO), and DKO mice treated with DMF (DKO + DMF) (n = 5 per genotype and condition). Spinal cord immunohistological sections processed for (A–C) Iba1, (D–F) GFAP, (G–I) synaptophysin, (J–L) APP, (M–O) Sudan Black, (P–R) 8-oxo-dG, (S–U) SMI-32, and (V–X) Cyt C. Representative images for (A, D, G, J, M, P, S, V) WT, (B, E, H, K, N, Q, T, W) DKO, and (C, F, I, L, O, R, U, X) DKO + DMF are shown. Scale bars = 125 μm (A–R) and 25 μm (S–X). Black arrows indicate APP or synaptophysin accumulations (H and K), and myelin debris (N) in DKO mice.

Y   Quantification of GFAP⁺ and Iba1⁺ cells per mm², and synaptophysin and APP accumulations in spinal cord immunohistological sections of WT (n = 5), DKO (n = 5), and DKO + DMF (n = 5) mice.

Z   Bar cross and treadmill tests performed on 18-month-old WT (n = 14), DKO (n = 16), and DKO + DMF (n = 14) mice. In the bar cross, data refer to number of slips and time (seconds) spent to cross the bar. In the treadmill test, data refer to number of shocks and time of shocks at the last time point measured (7 min and 30 s).

Data information: In (Y and Z), data are presented as mean ± SD. In (Y and Z), *P < 0.05, **P < 0.01, ***P < 0.001 (one-way ANOVA followed by Tukey's *post hoc* test), $P < 0.05, $$$P < 0.001 (non-parametric Kruskal–Wallis' test followed by Dunn's *post hoc* test). See the exact *P*-values in Appendix Table S3.
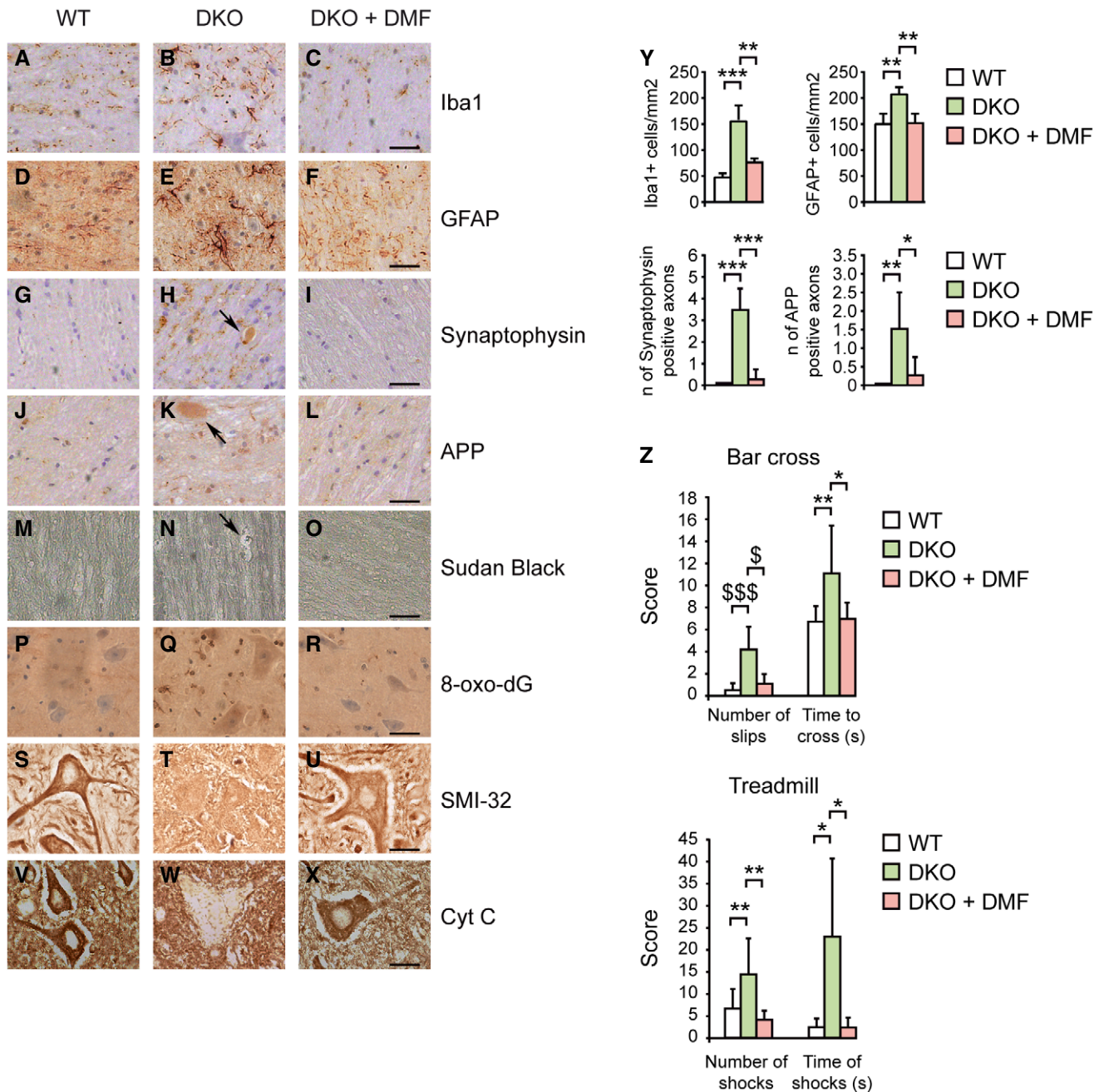
(Fig 5Z). As earlier described (Morato *et al*, 2015), DKO mice behaved worse than WT in the treadmill test, as the total number and duration of shocks were higher than in WT. Dimethyl fumarate treatment also ameliorated the performance of DKO mice in this test (Fig 5Z). In summary, these data indicate that DMF treatment halted the progression of the locomotor deficits observed in $Abcd1^-/Abcd2^{-/-}$ mice.

Discussion

In this work, we uncover an impaired AKT/GSK-3β/NRF2 axis in X-ALD, composed of a blunted NRF2-dependent response which obeys an aberrant upstream activation of GSK-3β. This impaired NRF2-dependent antioxidant response suggests a mechanism by which excess of C26:0 causes oxidative damage only in patients' fibroblasts in contrast with controls, even though both populations present similar amounts of ROS after C26:0 treatment (Fourcade *et al*, 2008). Indeed, the NRF2 target genes *Hmox1*, *Nqo1*, and *Gsta3*, whose expression we show is reduced in $Abcd1^-$ mice spinal cord, mediate a cellular defence against toxic, carcinogenic, and pharmacologically active electrophilic compounds (Lee *et al*, 2003; Dinkova-Kostova & Talalay, 2010). We propose that oxidative damage in this disease may be a consequence of the low activity of these enzymes, incapable of compensating for the increased ROS production. Inactivation of the NRF2 pathway is not a phenomenon limited to X-ALD, but is reported in several neurodegenerative disorders including Alzheimer's disease (Ramsey *et al*, 2007; Kanninen *et al*, 2008), amyotrophic lateral sclerosis (Sarlette *et al*, 2008), Friedrich's ataxia (Paupe *et al*, 2009; Shan *et al*, 2013), and experimental autoimmune encephalomyelitis mouse models (Morales Pantoja *et al*, 2016). A recent meta-analysis identified the NRF2 pathway as a common dysregulated hub in Alzheimer's and Parkinson's disease patients (Wang *et al*, 2017). Moreover, NRF2 can contribute to Parkinson's and Huntington's disease pathology (Johnson & Johnson, 2015). Indeed, NRF2-deficient mice are more vulnerable to striatal toxicity induced by systemic administration of 3-nitropropionic acid (3-NP) (Calkins *et al*, 2005), 1-methyl-4-phenyl-1,2,3,6 tetrahydropyridine (MPTP) (Burton *et al*, 2006; Chen *et al*, 2009), or 6-hydroxydopamine (6-OHDA) used to induce basal ganglia neural dysfunction (Jakel *et al*, 2007). Of note, NRF2-deficient mice also develop a more severe myelin oligodendrocyte glycoprotein (MOG)-induced experimental autoimmune encephalomyelitis with increased oxidative damage in the CNS, finally leading to enhanced demyelination and more pronounced axonal loss (Johnson *et al*, 2010). This provides a direct link between insufficient antioxidant response and axonal damage. Further, genetic variations in the NRF2 gene have been associated with risk and/or age of onset in amyotrophic lateral sclerosis, Alzheimer's, and Parkinson's disease (von Otter *et al*, 2010a,b; Bergstrom *et al*, 2014).

Glial cells are involved in the NRF2-mediated neuroprotective effects. *Ex vivo* studies and analysis of neurodegenerative models for motor neuron disorders, Parkinson's disease, or cerebral ischemia indicate that NRF2-mediated neuroprotection critically involves astrocyte-induced effects (Kraft *et al*, 2004; Shih *et al*, 2005; Chen *et al*, 2009). Initial evidence of the importance of NRF2 in glial cells comes from *Nrf2* knockout mice, which display astrogliosis and myelinopathy in the cerebellum (Hubbs *et al*, 2007). Also, striatum is protected from MPTP toxicity in transgenic mice which overexpress NRF2 in astrocytes (Chen *et al*, 2009).

Little is known about the link between AKT/GSK-3β and NRF2 in neurodegenerative diseases. Exacerbated GSK-3β activity is also present in other peroxisomal diseases, like rhizomelic chondrodysplasia punctata, in which plasmalogen deficiency leads to AKT inactivation and GSK-3β activation (da Silva *et al*, 2014). Future work should address and quantify both the functionality of the NRF2 pathway in rhizomelic chondrodysplasia punctata and the AKT/GSK-3β/NRF2 axis in other peroxisomal disorders, given the possibility of targeted treatments like DMF, for these metabolic diseases. Increased GSK-3β also occurs in other neurodegenerative conditions, like tauopathies, in which GSK-3β is one of the kinases responsible for pathological phosphorylation of Tau (Llorens-Martin *et al*, 2014); Parkinson's disease (Duka *et al*, 2009; Credle *et al*, 2015) or multiple sclerosis (Beurel *et al*, 2013).

In the present work, we inhibited GSK-3β in X-ALD fibroblasts using two different drugs, which restored NRF2 pathway function and activated transcription of NRF2 target genes upon oxidative stress. Thus, we reveal GSK-3β inhibition as a new therapeutic strategy in X-ALD, which is currently under investigation for other neurodegenerative diseases. In the Senescence Accelerated Mouse-Prone 8 (SAMP8) mouse, an Alzheimer's disease mouse model, GSK-3β inhibition caused NRF2 activation and decreased oxidative stress, together with reduced Tau phosphorylation and improved learning and memory (Farr *et al*, 2014). Another study uncovered the therapeutic potential of GSK-3β pathway inhibition to restore neurodevelopmental defects in hereditary spastic paraplegia (HSP) patients with SPG11 mutations (Mishra *et al*, 2016). Pathways that modulate GSK-3β, such as phosphoinositide 3-kinase (PI3K)/AKT and WNT/β-catenin, also regulate myelination (Fancy *et al*, 2009; Guo *et al*, 2016). Unfortunately, GSK-3 inhibitors have so far met little success in clinical trials for neurodegenerative diseases. Two phase II clinical trials with the GSK-3β inhibitor, Tideglusib, showed no clinical benefits in Alzheimer's disease (Lovestone *et al*, 2015) and progressive supranuclear palsy (Tolosa *et al*, 2014). We therefore chose DMF to activate NRF2 in our X-ALD preclinical models using a similar dosage to that administered to human multiple sclerosis patients, paving the way to clinical translation. DMF treatment is advantageous because it enhances the NRF2 antioxidant pathway, but also exerts pleiotropic effects improving proteostasis, mitochondrial function, and neuroinflammation (Johnson & Johnson, 2015), cellular responses that also contribute to the pathogenesis of adrenoleukodystrophy (Fourcade *et al*, 2015). Indeed, previous *in vitro* studies described the effects of DMF on mitochondrial function (Scannevin *et al*, 2012; Ahuja *et al*, 2016; Peng *et al*, 2016). Here, we describe a positive effect of DMF on mitochondrial biogenesis and function in the central nervous system *in vivo*, characterized by increased mtDNA levels and mitochondrial biogenesis regulatory gene expression (*Sirt1*, *Ppargc1a*, *Nrf1*, *Tfam*), as well as normalized ATP levels in the spinal cord of $Abcd1^-$ mice. These results are supported by recent data in mice and multiple sclerosis patients treated with DMF (Hayashi *et al*, 2017).

Neuroinflammation is another common feature of neurodegenerative diseases. In this study, we observed normalization in the gene expression of *Nfkb2* transcription factor and pro-inflammatory cytokines like *Tnfa*, *Ccl5*, *Cxcl10*, and *Ccr6*, concomitant with an increase in the anti-inflammatory cytokines *Il10* and *Chil3*. This DMF effect is consistent with previous reports showing an *in vivo* anti-inflammatory effect in the experimental autoimmune encephalomyelitis animal model (Schilling *et al*, 2006). We also

show that DMF prevented microgliosis and astrocytosis in *Abcd1*⁻/*Abcd2*⁻/⁻ mice, consistent with results from recent studies in Parkinson's disease mouse models (Jing *et al*, 2015; Lastres-Becker *et al*, 2016). NRF2 activation also occurs in PBMC and glial cells from multiple sclerosis patients treated with DMF from the DEFINE and CONFIRM studies (Gopal *et al*, 2017). Yet, the immunomodulatory effect of DMF in the nervous system can be NRF2-dependent (Linker *et al*, 2011) or independent (Brennan *et al*, 2016). G protein-coupled receptor 109A (GPR109A), also known as the hydroxycarboxylic acid receptor 2 (HCA2), is another DMF target (Parodi *et al*, 2015). Future studies on the role of HCA2 in X-ALD and other demyelinating diseases will further enlighten the mechanism of action of DMF in the neuroinflammatory axis.

In view of these data, DMF exhibits a great potential to treat X-ALD and other neurodegenerative diseases with an overall good safety profile (Fox *et al*, 2012; Gold *et al*, 2012). However, some precautions need to be observed with this drug, as side effects need to be monitored and evaluated carefully. The most important is lymphocytopenia (Fox *et al*, 2016). Of > 230,000 patients treated with DMF in the period of 3 years following commercial availability, five cases of progressive multifocal leukoencephalopathy (PML) have been reported, in the setting of moderate to severe prolonged lymphocytopenia (Pardo & Jones, 2017). As a consequence, FDA and EMA (EMA/627077/2015) recently issued updated safety recommendations to minimize PML risk, which include regular blood counts. Recent reports indicate that a reduction in T cells rather than a general reduction in lymphocyte count may be associated with these cases (Gieselbach *et al*, 2017), which still represent a very low percentage of all the patients treated with fumaric acid esters.

In summary, our data uncover a novel role of GSK-3β/NRF2 in the physiopathogenesis of X-ALD. By identifying the mechanism impaired in the endogenous antioxidant response in this disease, we reveal a novel therapeutic intervention using DMF treatment to overcome the molecular pathogenesis and clinical signs of adrenoleukodystrophy in the mouse. Our data provide strong rationale to propose phase II clinical trials with DMF in adrenoleukodystrophy patients.

Materials and Methods

Reagents and antibodies

The following chemicals were used: DMF (Ref. 242926), hexacosanoic acid (C26:0, Ref. H0388), and oligomycin (Ref. O4876) were purchased from Sigma-Aldrich (Steinheim, Germany). GSK-3β inhibitors CHIR99021 (6-[[2-[[4-(2,4-dichlorophenyl)-5-(5-methyl-1H-imidazol-2-yl)-2-pyrimidinyl]amino]ethyl]amino]-3-pyridinecarbonitrile; Ref. 361559) and SB216763 (3-(2,4-dichlorophenyl)-4-(1-methyl-1H-indol-3-yl)-1H-pyrrole-2,5-dione; Ref. 1616) were purchased from Calbiochem (Billerica, MA, USA) and Tocris Biosciences (Bristol, UK), respectively. Detailed information on antibodies is summarized in Appendix Table S1.

Mouse experiments

We used male mice of a pure C57BL/6J background. All methods employed in this study were in accordance with the ARRIVE guidelines, the Guide for the Care and Use of Laboratory Animals (Guide, 8th edition, 2011, NIH) and European (2010/63/UE) and Spanish (RD 53/2013) legislation. Experimental protocols were approved by IDIBELL, IACUC (Institutional Animal Care and Use Committee), and regional authority (3546 DMAH, Generalitat de Catalunya, Spain). IDIBELL animal facility is accredited by The Association for Assessment and Accreditation of Laboratory Animal Care (AAALAC, Unit 1155). Animals were housed at 22°C on specific pathogen-free conditions, in a 12-h light/dark cycle, and *ad libitum* access to food and water. Cages contained three to four animals.

We used two X-ALD mouse models in this study. We evaluated the biochemical signs of adult X-ALD in *Abcd1*⁻ mice at 12 months of age. These mice present oxidative stress (Fourcade *et al*, 2008) and energetic homeostasis impairment (Galino *et al*, 2011) before the first clinical signs of adrenomyeloneuropathy-like pathology (axonopathy and locomotor impairment) appear at 20 months (Pujol *et al*, 2002).

To address the therapeutic effect of DMF, we assessed the clinical signs of adrenomyeloneuropathy in *Abcd1*⁻/*Abcd2*⁻/⁻ (DKO) mice, which display increased VLCFA accumulation in the spinal cord (Pujol *et al*, 2004), higher levels of oxidative damage to proteins (Fourcade *et al*, 2008; Galino *et al*, 2011), and a more severe adrenomyeloneuropathy-like pathology with an earlier onset at 12 months of age (Pujol *et al*, 2004). These mice are the preferred X-ALD mouse model for therapeutic testing (Mastroeni *et al*, 2009; Lopez-Erauskin *et al*, 2011; Morato *et al*, 2013, 2015; Launay *et al*, 2015, 2017).

For biochemical analysis, we euthanized the mice and stored the tissues at −80°C after snap-freezing them in liquid nitrogen. For histological analysis, spinal cord was harvested from 18-month-old mice after perfusing them with 4% paraformaldehyde (PFA; Sigma-Aldrich, Ref. 441244) in 0.1 M phosphate buffer pH 7.4. Histological and behavioral experiments were performed in a blind manner with respect to the animal's genotype and the treatment administered.

DMF administration to mice

Dimethyl fumarate was mixed into AIN-76A chow from Dyets (Bethlehem, PA, USA) to provide a dose of 100 mg/kg/day. Human equivalent dose would be 8 mg/kg/day (240 mg in a typical 60 kg person). This is equivalent to the starting dose of BG-12/Tecfidera for multiple sclerosis patients, 120 mg twice a day (EMA/204830/2013).

To characterize biochemical signs in adult X-ALD mice, 8-month-old animals were randomly assigned to one of the following dietary groups for 4 months. Group I: WT mice received normal AIN-76A chow (*n* = 12); group II: *Abcd1*⁻ mice received normal AIN-76A chow (*n* = 12); group III: *Abcd1*⁻ mice received AIN-76A chow containing DMF (*n* = 12). To evaluate the effect of DMF on the clinical signs of adrenomyeloneuropathy-like pathology, 12-month-old animals were randomly assigned to one of the following dietary groups for 6 months. Group I: WT mice received normal AIN-76A chow (*n* = 14); group II: *Abcd1*⁻/*Abcd2*⁻/⁻ mice received normal AIN-76A chow (*n* = 16); and group III: *Abcd1*⁻/*Abcd2*⁻/⁻ mice received AIN-76A chow containing DMF (*n* = 14). DMF had no effect on weight or food intake under any treatment protocol, and none of the mice administered with DMF experienced any adverse events or death during the treatment.

Human samples

Primary human fibroblasts were prepared from skin biopsies collected from healthy individuals ($n = 8$) and adrenomyeloneuropathy patients ($n = 8$) according to the IDIBELL guidelines for sampling, including informed consent obtained from the persons involved or their representatives according to the Declaration of Helsinki and approved by the ethical committee of IDIBELL.

The fibroblasts were grown in Dulbecco's modified Eagle's medium (Gibco, Thermo Fisher Scientific Inc., Rockford, IL, USA) containing 10% fetal bovine serum (Cultek, Ref. 91S1800; Madrid, Spain), 100 U/ml penicillin, and 100 μg/ml streptomycin (Pen Strep; Gibco, Ref. 15140-122) and maintained at 37°C in a humidified 95% air/5% CO_2 incubator. The compounds tested were added at 80–90% cell confluence. 15 μM oligomycin and 50 μM C26:0 were diluted in ethanol and added for 18 and 24 h, respectively. DMF (20 μM), dissolved in ethanol, and GSK-3β inhibitors (CHIR99021 at 3 μM and SB216763 at 10 μM), dissolved in dimethylsulfoxide (DMSO), were added 18 h after C26:0 treatment for 6 h. All experiments were performed with fibroblasts at passage 10–20.

Nuclear-cytoplasmic fractionation in human fibroblasts

We performed subcellular fractionation to study NRF2 translocation to the nucleus, using a non-ionic detergent lysis method with slight modifications (Abmayr *et al*, 2006). Briefly, cells grown in 100 mm diameter dishes (Nunc Dish, Thermo Fisher Inc.) were washed in ice-cold phosphate buffer saline (PBS) pH 7.4 and collected by trypsinization (0.25% Trypsin-EDTA Solution A; Biological Industries USA, Cromwell, CT, USA) in a 15-ml falcon tube. After centrifugation and a new ice-cold PBS wash, the cell pellet was resuspended with 140 μl of lysis buffer (0.1% Nonidet P-40 in PBS, plus proteases (Complete Mini, Ref. 11836153001; Roche Diagnostics GmbH; Mannheim; Germany) and phosphatases (PhosSTOP, Ref. 04906845001; Roche Diagnostics GmbH) inhibitors) and scratched 20 times to lyse the cells. After 10-min incubation on ice, we centrifuged at 300 *g* during 5 min at 4°C in an Eppendorf® microcentrifuge. Supernatant was collected as cytoplasmic fraction. Then, we added 70 μl of RIPA buffer (50 mM Tris pH 8.0, 150 mM NaCl, 12 mM deoxycholic acid, and 1% Nonidet P-40; complemented with protease/phosphatase inhibitors) to the pellet to obtain the nuclear fraction. After homogenizing the pellet through a syringe with a 25G needle and 30 min of shaking at 4°C, we centrifuged for 10 min at 16,100 *g* at 4°C. Supernatant was collected as nuclear fraction. Then, we performed immunoblot procedures as described below. Lamin B1 and aldolase A were used as markers for nuclear and cytoplasmic fraction, respectively.

Quantitative real-time PCR

RNA extraction and retrotranscription into cDNA, DNA extraction and quantitative RT–PCR analysis were performed as previously described (Morato *et al*, 2013). Total RNA was extracted from human fibroblasts and mouse tissues using RNeasy Kit (Qiagen, Hilden, Germany). Total DNA was extracted from mouse spinal cord using Gentra Puregene Tissue Kit (Qiagen, Hilden, Germany). The expression of the genes of interest was analyzed by Q–PCR using

TaqMan® Gene Expression Assays (Thermo Fisher Scientific Inc.) and standardized TaqMan® probes (Appendix Table S2) on a LightCycler® 480 Real-Time PCR System (Roche Diagnostics GmbH). Relative quantification was carried out using the "Delta-Delta Ct" (ΔΔCt) method with *Rplp0* as endogenous control. To quantify mouse mitochondrial DNA (mtDNA) content, primers for mouse cytochrome b (*Cytb*) were designed (Custom TaqMan Gene Expression Assays; Thermo Fisher Scientific Inc.). The sequences for *Cytb* primers were as follows: ATGACCCCAATACGCAAAATTA (forward) and GGAGGACATAGCCTATGAAGG (reverse), and the FAM-labeled probe sequence was TTGCAACTATAGCAACAG. Quantification of mtDNA was referred to nuclear DNA (nDNA), determined by the amplification of the intron-less mouse nuclear gene *Cebpa* (Morato *et al*, 2013). Transcript quantification was performed in triplicate for each sample.

Immunoblot

Human fibroblasts and mouse tissues were homogenized in RIPA buffer and then sonicated, centrifuged, and heated for 10 min at 70°C after adding 4X NuPAGE® LDS Sample Buffer (Invitrogen, Thermo Fisher Scientific Inc.). 20–50 μg of proteins was loaded onto 8% Novex NuPAGE® SDS–PAGE gel system (Invitrogen, Thermo Fisher Scientific Inc.) and run for 60–90 min at 120 V in NuPAGE® MOPS SDS Running Buffer (Invitrogen, Thermo Fisher Scientific Inc.) supplemented with 5 mM sodium bisulfite (Ref. 243973, Sigma-Aldrich). SeeBlue® Plus2 Pre-stained (Invitrogen, Thermo Fisher Scientific Inc.) was used as a ladder.

Regarding the different AKT or GSK-3β phosphorylations, we run the same quantity of samples (processed at the same time) in several gels in parallel, always performing Ponceau staining and Y-tubulin immunoblotting to confirm equal loading. Resolved proteins were transferred onto nitrocellulose membranes using iBlot® 2 Gel Transfer Device (Invitrogen, Thermo Fisher Scientific Inc.). After blocking in 5% bovine serum albumin (BSA, Sigma-Aldrich) in 0.05% TBS-Tween (TBS-T) for 1 h at room temperature, membranes were incubated with corresponding diluted primary antibodies (Appendix Table S1) in 5% BSA in 0.05% TBS-T overnight at 4°C. Following incubation with diluted secondary antibody (Appendix Table S1) in 0.05% TBS-T for 1 h at room temperature, proteins were detected with ECL Western blotting analysis system (GE Healthcare, Buckinghamshire, UK), followed by exposure to CL-XPosure Film (Thermo Fisher Scientific Inc.) as earlier described (Galino *et al*, 2011). It is worth noting that the correct band for NRF2 is at 100 kDa, not at the predicted 68 kDa (Lau *et al*, 2013). Immunoblots were quantified by densitometry using ImageJ v1.50i (U. S. National Institutes of Health, Bethesda, MD, USA).

ATP

ATP levels were measured by a chemiluminescence system using ATPlite 1step (PerkinElmer, Inc., Waltham, MA, USA), as already described (Galino *et al*, 2011).

Evaluation of oxidative lesions

AASA, CML, CEL, and MDAL concentrations in total proteins from spinal cord homogenates were measured by gas chromatography/

mass spectrometry (GC/MS), as reported (Fourcade *et al*, 2008). The amounts of products were expressed as the ratio of micromole of AASA, CML, CEL, or MDAL per mol of lysine.

Measurement of very long-chain fatty acids

Content of very long-chain fatty acids in total lipids from spinal cord was analyzed as methyl ester derivative by gas chromatography, as described before (Morato *et al*, 2013). Briefly, separation was performed by a DBWAX capillary column (30 m × 0.25 mm × 0.20 μm) in a GC System 7890A with a Series Injector 7683B and a FID detector (Agilent Technologies). The injection port was maintained at 220°C, and the detector at 250°C; the temperature program was 5 min at 145°C, then 2°C/min to 240°C with a hold of 10 min, then 0.5°C/min to 250°C, and finally hold at 250°C for 5 min. Identification of fatty acid methyl esters was made by comparison with authentic standards (Sigma and Larodan Fine Chemicals). Results are represented as fold change to WT mice.

Immunohistochemistry

Spinal cords were embedded in paraffin, and serial sections (4 μm thick) were cut in a transversal or longitudinal (1 cm long) plane after perfusion with 4% PFA. Immunohistochemistry (IHC) studies performed in WT, *Abcd1⁻/Abcd2⁻/⁻* (DKO), and *Abcd1⁻/Abcd2⁻/⁻* mice treated with DMF (DKO+DMF) were carried out using the avidin–biotin peroxidase method, as reported earlier (Launay *et al*, 2015).

After primary antibody incubation, the sections were incubated with the Labelled Streptavidin-Biotin2 System (LSAB2, Ref. K0675, Dako). Staining was visualized after incubation with 3,3′-diaminobenzidine (DAB) substrate chromogen (Ref. D5637, Sigma-Aldrich), which results in a brown-colored precipitate at the antigen site. After dehydrating the sections, slides were mounted with DPX (Ref. 06522, Sigma-Aldrich).

Images were acquired using Olympus BX51 microscope (20x/N.A 0.50 Ph 1 UPlan FL N; Olympus Corporation, Tokyo, Japan) connected to an Olympus DP71 camera and Cell^B software (Olympus Corporation). The researcher was blinded to both genotype and treatment of the sample when analyzing the results. The number of GFAP⁺ cells (astrocytes) and Iba1⁺ cells (microglia) per mm² was determined in the spinal cord's ventral horn of WT, *Abcd1⁻/Abcd2⁻/⁻*, and DMF-treated *Abcd1⁻/Abcd2⁻/⁻* mice (*n* = 5). The number of brown-colored cells was considered and counted with Cell Counter ImageJ plugin. Data are presented as an average of two 20× images per animal for each group.

Analysis of locomotion

Locomotor deficits were assessed with the bar cross test and the treadmill test, as already described (Morato *et al*, 2013).

Statistical analysis

Sample size was chosen according to previous experience in the laboratory, in similar experiments with long-term oral treatments that were performed with the same animal model. No animals were excluded from analysis. Animals and samples were allocated to

The paper explained

Problem
X-linked adrenoleukodystrophy (X-ALD) is a rare disease that met the public eye in the early 90s thanks to the movie Lorenzo's Oil which has, despite recent advances in gene therapy, still no satisfactory treatment for most cases. The underlying genetic defect causes the malfunction of the fatty acid transporter ABCD1. Because early hallmarks of X-ALD are oxidative damage and bioenergetic impairment, here we evaluated the endogenous antioxidant response seeking for suitable drug targets.

Results
Using mouse models of X-ALD and cells obtained from the skin of X-ALD patients, we uncovered an impaired NRF2 antioxidant response caused by aberrant activity of GSK-3β, a kinase upstream in this cascade. We found that GSK-3β inhibitors reactivated the blunted NRF2 response in patients' fibroblasts. In the mouse models (*Abcd1⁻* and *Abcd1⁻/Abcd2⁻/⁻* mice), oral administration of dimethyl fumarate (DMF/BG12/Tecfidera), an FDA-approved NRF2 activator, normalized molecular defects relative to ABCD1 deficiency such as (i) oxidative damage, (ii) mitochondrial depletion and bioenergetic failure, and (iii) neuroinflammation. Moreover, DMF halted axonal degeneration and locomotor disability in the mouse model.

Impact
This preclinical study identifies a druggable pathway underlying axonal degeneration in X-ALD and paves the way to use dimethyl fumarate in phase II clinical trials. The study highlights as well the potential of drugs targeting the GSK-3β/NRF2 axis for other axonal disorders with shared pathomechanisms.

different treatment groups by randomization. Researchers were blinded to the group assignment and to the animal number when performing the locomotor experiments until the data were processed for statistical analysis.

The values were expressed as the mean ± standard deviation (SD). The significant differences when comparing two groups were determined by a two-tailed unpaired Student's *t*-test (*P < 0.05, **P < 0.01, ***P < 0.001). When comparing more than two groups, significant differences were determined by one-way ANOVA followed by Tukey's/Dunnett's *post hoc* tests (*/#*P* < 0.05, **/##*P* < 0.01, ***/###*P* < 0.001) or Kruskal–Wallis non-parametric test followed by Dunn's *post hoc* test (\$*P* < 0.05, \$\$*P* < 0.01, \$\$\$*P* < 0.001), after verifying normality (Shapiro–Wilk test). Statistical analyses were performed using SPSS for Windows version 12.0.

Author contributions

Conflict of interest

For more information

(i) X-ALD in OMIM: http://omim.org/entry/300100

(ii) X-ALD database: http://adrenoleukodystrophy.info

(iii) European Leukodystrophy Association: http://ela-asso.com/en/

(iv) Author's website: http://www.neurometabolic-lab.org/

References

Abmayr SM, Yao T, Parmely T, Workman JL (2006) Preparation of nuclear and cytoplasmic extracts from mammalian cells. *Curr Protoc Mol Biol* Chapter 12: Unit 12.11

Ahuja M, Ammal Kaidery N, Yang L, Calingasan N, Smirnova N, Gaisin A, Gaisina IN, Gazaryan I, Hushpulian DM, Kaddour-Djebbar I *et al* (2016) Distinct Nrf2 signaling mechanisms of fumaric acid esters and their role in neuroprotection against 1-Methyl-4-Phenyl-1,2,3,6-tetrahydropyridine-induced experimental parkinson's-like disease. *J Neurosci* 36: 6332–6351

van de Beek MC, Ofman R, Dijkstra I, Wijburg F, Engelen M, Wanders R, Kemp S (2017) Lipid-induced endoplasmic reticulum stress in X-linked adrenoleukodystrophy. *Biochim Biophys Acta* 1863: 2255–2265

Berger J, Molzer B, Fae I, Bernheimer H (1994) X-linked adrenoleukodystrophy (ALD): a novel mutation of the ALD gene in 6 members of a family presenting with 5 different phenotypes. *Biochem Biophys Res Commun* 205: 1638–1643

Bergstrom P, von Otter M, Nilsson S, Nilsson AC, Nilsson M, Andersen PM, Hammarsten O, Zetterberg H (2014) Association of NFE2L2 and KEAP1 haplotypes with amyotrophic lateral sclerosis. *Amyotroph Lateral Scler Frontotemporal Degener* 15: 130–137

Beurel E, Kaidanovich-Beilin O, Yeh WI, Song L, Palomo V, Michalek SM, Woodgett JR, Harrington LE, Eldar-Finkelman H, Martinez A *et al* (2013) Regulation of Th1 cells and experimental autoimmune encephalomyelitis by glycogen synthase kinase-3. *J Immunol* 190: 5000–5011

Brennan MS, Patel H, Allaire N, Thai A, Cullen P, Ryan S, Lukashev M, Bista P, Huang R, Rhodes KJ *et al* (2016) Pharmacodynamics of dimethyl fumarate are tissue specific and involve NRF2-dependent and -independent mechanisms. *Antioxid Redox Signal* 24: 1058–1071

Burton NC, Kensler TW, Guilarte TR (2006) *In vivo* modulation of the Parkinsonian phenotype by Nrf2. *Neurotoxicology* 27: 1094–1100

Calkins MJ, Jakel RJ, Johnson DA, Chan K, Kan YW, Johnson JA (2005) Protection from mitochondrial complex II inhibition *in vitro* and *in vivo* by Nrf2-mediated transcription. *Proc Natl Acad Sci USA* 102: 244–249

Cartier N, Hacein-Bey-Abina S, Bartholomae CC, Veres G, Schmidt M, Kutschera I, Vidaud M, Abel U, Dal-Cortivo L, Caccavelli L *et al* (2009) Hematopoietic stem cell gene therapy with a lentiviral vector in X-linked adrenoleukodystrophy. *Science* 326: 818–823

Chen PC, Vargas MR, Pani AK, Smeyne RJ, Johnson DA, Kan YW, Johnson JA (2009) Nrf2-mediated neuroprotection in the MPTP mouse model of Parkinson's disease: critical role for the astrocyte. *Proc Natl Acad Sci USA* 106: 2933–2938

Coghlan MP, Culbert AA, Cross DA, Corcoran SL, Yates JW, Pearce NJ, Rausch OL, Murphy GJ, Carter PS, Roxbee Cox L *et al* (2000) Selective small molecule inhibitors of glycogen synthase kinase-3 modulate glycogen metabolism and gene transcription. *Chem Biol* 7: 793–803

Credle JJ, George JL, Wills J, Duka V, Shah K, Lee YC, Rodriguez O, Simkins T, Winter M, Moechars D *et al* (2015) GSK-3beta dysregulation contributes to parkinson's-like pathophysiology with associated region-specific phosphorylation and accumulation of tau and alpha-synuclein. *Cell Death Differ* 22: 838–851

Dinkova-Kostova AT, Talalay P (2010) NAD(P)H:quinone acceptor oxidoreductase 1 (NQO1), a multifunctional antioxidant enzyme and exceptionally versatile cytoprotector. *Arch Biochem Biophys* 501: 116–123

Duka T, Duka V, Joyce JN, Sidhu A (2009) Alpha-Synuclein contributes to GSK-3beta-catalyzed Tau phosphorylation in Parkinson's disease models. *FASEB J* 23: 2820–2830

Eichler F, Duncan C, Musolino PL, Orchard PJ, De Oliveira S, Thrasher AJ, Armant M, Dansereau C, Lund TC, Miller WP *et al* (2017) Hematopoietic stem-cell gene therapy for cerebral adrenoleukodystrophy. *N Engl J Med* 377: 1630–1638

Ellrichmann G, Petrasch-Parwez E, Lee DH, Reick C, Arning L, Saft C, Gold R, Linker RA (2011) Efficacy of fumaric acid esters in the R6/2 and YAC128 models of Huntington's disease. *PLoS One* 6: e16172

Engelen M, Kemp S, de Visser M, van Geel BM, Wanders RJ, Aubourg P, Poll-The BT (2012) X-linked adrenoleukodystrophy (X-ALD): clinical presentation and guidelines for diagnosis, follow-up and management. *Orphanet J Rare Dis* 7: 51

Engelen M, Barbier M, Dijkstra IM, Schur R, de Bie RM, Verhamme C, Dijkgraaf MG, Aubourg PA, Wanders RJ, van Geel BM *et al* (2014) X-linked adrenoleukodystrophy in women: a cross-sectional cohort study. *Brain* 137: 693–706

Fancy SP, Baranzini SE, Zhao C, Yuk DI, Irvine KA, Kaing S, Sanai N, Franklin RJ, Rowitch DH (2009) Dysregulation of the Wnt pathway inhibits timely myelination and remyelination in the mammalian CNS. *Genes Dev* 23: 1571–1585

Farr SA, Ripley JL, Sultana R, Zhang Z, Niehoff ML, Platt TL, Murphy MP, Morley JE, Kumar V, Butterfield DA (2014) Antisense oligonucleotide against GSK-3beta in brain of SAMP8 mice improves learning and memory and decreases oxidative stress: involvement of transcription factor Nrf2 and implications for Alzheimer disease. *Free Radic Biol Med* 67: 387–395

Fourcade S, Lopez-Erauskin J, Galino J, Duval C, Naudi A, Jove M, Kemp S, Villarroya F, Ferrer I, Pamplona R *et al* (2008) Early oxidative damage underlying neurodegeneration in X-adrenoleukodystrophy. *Hum Mol Genet* 17: 1762–1773

Fourcade S, Ruiz M, Camps C, Schluter A, Houten SM, Mooyer PA, Pampols T, Dacremont G, Wanders RJ, Giros M *et al* (2009) A key role for the peroxisomal ABCD2 transporter in fatty acid homeostasis. *Am J Physiol Endocrinol Metab* 296: E211–E221

Fourcade S, Ruiz M, Guilera C, Hahnen E, Brichta L, Naudi A, Portero-Otin M, Dacremont G, Cartier N, Wanders R *et al* (2010) Valproic acid induces

antioxidant effects in X-linked adrenoleukodystrophy. *Hum Mol Genet* 19: 2005–2014

Fourcade S, Ferrer I, Pujol A (2015) Oxidative stress, mitochondrial and proteostasis malfunction in adrenoleukodystrophy: a paradigm for axonal degeneration. *Free Radic Biol Med* 88: 18–29

Fox RJ, Miller DH, Phillips JT, Hutchinson M, Havrdova E, Kita M, Yang M, Raghupathi K, Novas M, Sweetser MT *et al* (2012) Placebo-controlled phase 3 study of oral BG-12 or glatiramer in multiple sclerosis. *N Engl J Med* 367: 1087–1097

Fox RJ, Chan A, Gold R, Phillips JT, Selmaj K, Chang I, Novas M, Rana J, Marantz JL (2016) Characterizing absolute lymphocyte count profiles in dimethyl fumarate-treated patients with MS: patient management considerations. *Neurol Clin Pract* 6: 220–229

Galino J, Ruiz M, Fourcade S, Schluter A, Lopez-Erauskin J, Guilera C, Jove M, Naudi A, Garcia-Arumi E, Andreu AL *et al* (2011) Oxidative damage compromises energy metabolism in the axonal degeneration mouse model of x-adrenoleukodystrophy. *Antioxid Redox Signal* 15: 2095–2107

Gieselbach RJ, Muller-Hansma AH, Wijburg MT, de Bruin-Weller MS, van Oosten BW, Nieuwkamp DJ, Coenjaerts FE, Wattjes MP, Murk JL (2017) Progressive multifocal leukoencephalopathy in patients treated with fumaric acid esters: a review of 19 cases. *J Neurol* 264: 1155–1164

Gold R, Kappos L, Arnold DL, Bar-Or A, Giovannoni G, Selmaj K, Tornatore C, Sweetser MT, Yang M, Sheikh SI *et al* (2012) Placebo-controlled phase 3 study of oral BG-12 for relapsing multiple sclerosis. *N Engl J Med* 367: 1098–1107

Gopal S, Mikulskis A, Gold R, Fox RJ, Dawson KT, Amaravadi L (2017) Evidence of activation of the Nrf2 pathway in multiple sclerosis patients treated with delayed-release dimethyl fumarate in the Phase 3 DEFINE and CONFIRM studies. *Mult Scler* 23: 1875–1883

Guo X, Snider WD, Chen B (2016) GSK3beta regulates AKT-induced central nervous system axon regeneration via an eIF2Bepsilon-dependent, mTORC1-independent pathway. *Elife* 5: e11903

Hayashi G, Jasoliya M, Sahdeo S, Saccà F, Pane C, Filla A, Marsili A, Puorro G, Lanzillo R, Brescia Morra V *et al* (2017) Dimethyl fumarate mediates Nrf2-dependent mitochondrial biogenesis in mice and humans. *Hum Mol Genet* 26: 2864–2873

Hein S, Schonfeld P, Kahlert S, Reiser G (2008) Toxic effects of X-linked adrenoleukodystrophy-associated, very long chain fatty acids on glial cells and neurons from rat hippocampus in culture. *Hum Mol Genet* 17: 1750–1761

Holmstrom KM, Baird L, Zhang Y, Hargreaves I, Chalasani A, Land JM, Stanyer L, Yamamoto M, Dinkova-Kostova AT, Abramov AY (2013) Nrf2 impacts cellular bioenergetics by controlling substrate availability for mitochondrial respiration. *Biol Open* 2: 761–770

Hubbs AF, Benkovic SA, Miller DB, O'Callaghan JP, Battelli L, Schwegler-Berry D, Ma Q (2007) Vacuolar leukoencephalopathy with widespread astrogliosis in mice lacking transcription factor Nrf2. *Am J Pathol* 170: 2068–2076

Innamorato NG, Rojo AI, Garcia-Yague AJ, Yamamoto M, de Ceballos ML, Cuadrado A (2008) The transcription factor Nrf2 Is a therapeutic target against brain inflammation. *J Immunol* 181: 680–689

Itoh K, Chiba T, Takahashi S, Ishii T, Igarashi K, Katoh Y, Oyake T, Hayashi N, Satoh K, Hatayama I *et al* (1997) An Nrf2/small Maf heterodimer mediates the induction of phase II detoxifying enzyme genes through antioxidant response elements. *Biochem Biophys Res Commun* 236: 313–322

Jakel RJ, Townsend JA, Kraft AD, Johnson JA (2007) Nrf2-mediated protection against 6-hydroxydopamine. *Brain Res* 1144: 192–201

Jing X, Shi H, Zhang C, Ren M, Han M, Wei X, Zhang X, Lou H (2015) Dimethyl fumarate attenuates 6-OHDA-induced neurotoxicity in SH-SY5Y cells and in animal model of Parkinson's disease by enhancing Nrf2 activity. *Neuroscience* 286: 131–140

Johnson DA, Amirahmadi S, Ward C, Fabry Z, Johnson JA (2010) The absence of the pro-antioxidant transcription factor Nrf2 exacerbates experimental autoimmune encephalomyelitis. *Toxicol Sci* 114: 237–246

Johnson DA, Johnson JA (2015) Nrf2–a therapeutic target for the treatment of neurodegenerative diseases. *Free Radic Biol Med* 88: 253–267

Kaidery NA, Banerjee R, Yang L, Smirnova NA, Hushpulian DM, Liby KT, Williams CR, Yamamoto M, Kensler TW, Ratan RR *et al* (2013) Targeting Nrf2-mediated gene transcription by extremely potent synthetic triterpenoids attenuate dopaminergic neurotoxicity in the MPTP mouse model of Parkinson's disease. *Antioxid Redox Signal* 18: 139–157

Kanninen K, Malm TM, Jyrkkanen HK, Goldsteins G, Keksa-Goldsteine V, Tanila H, Yamamoto M, Yla-Herttuala S, Levonen AL, Koistinaho J (2008) Nuclear factor erythroid 2-related factor 2 protects against beta amyloid. *Mol Cell Neurosci* 39: 302–313

Kanninen K, Heikkinen R, Malm T, Rolova T, Kuhmonen S, Leinonen H, Yla-Herttuala S, Tanila H, Levonen AL, Koistinaho M *et al* (2009) Intrahippocampal injection of a lentiviral vector expressing Nrf2 improves spatial learning in a mouse model of Alzheimer's disease. *Proc Natl Acad Sci USA* 106: 16505–16510

Kemper AR, Brosco J, Comeau AM, Green NS, Grosse SD, Jones E, Kwon JM, Lam WK, Ojodu J, Prosser LA *et al* (2017) Newborn screening for X-linked adrenoleukodystrophy: evidence summary and advisory committee recommendation. *Genet Med* 19: 121–126

Komatsu M, Kurokawa H, Waguri S, Taguchi K, Kobayashi A, Ichimura Y, Sou YS, Ueno I, Sakamoto A, Tong KI *et al* (2010) The selective autophagy substrate p62 activates the stress responsive transcription factor Nrf2 through inactivation of Keap1. *Nat Cell Biol* 12: 213–223

Kraft AD, Johnson DA, Johnson JA (2004) Nuclear factor E2-related factor 2-dependent antioxidant response element activation by tert-butylhydroquinone and sulforaphane occurring preferentially in astrocytes conditions neurons against oxidative insult. *J Neurosci* 24: 1101–1112

Lastres-Becker I, Garcia-Yague AJ, Scannevin RH, Casarejos MJ, Kugler S, Rabano A, Cuadrado A (2016) Repurposing the NRF2 activator dimethyl fumarate as therapy against synucleinopathy in Parkinson's disease. *Antioxid Redox Signal* 25: 61–77

Lau A, Tian W, Whitman SA, Zhang DD (2013) The predicted molecular weight of Nrf2: it is what it is not. *Antioxid Redox Signal* 18: 91–93

Launay N, Ruiz M, Fourcade S, Schluter A, Guilera C, Ferrer I, Knecht E, Pujol A (2013) Oxidative stress regulates the ubiquitin-proteasome system and immunoproteasome functioning in a mouse model of X-adrenoleukodystrophy. *Brain* 136: 891–904

Launay N, Aguado C, Fourcade S, Ruiz M, Grau L, Riera J, Guilera C, Giros M, Ferrer I, Knecht E *et al* (2015) Autophagy induction halts axonal degeneration in a mouse model of X-adrenoleukodystrophy. *Acta Neuropathol* 129: 399–415

Launay N, Ruiz M, Grau L, Ortega FJ, Ilieva EV, Martinez JJ, Galea E, Ferrer I, Knecht E, Pujol A *et al* (2017) Tauroursodeoxycholic bile acid arrests axonal degeneration by inhibiting the unfolded protein response in X-linked adrenoleukodystrophy. *Acta Neuropathol* 133: 283–301

Lee JM, Calkins MJ, Chan K, Kan YW, Johnson JA (2003) Identification of the NF-E2-related factor-2-dependent genes conferring protection against oxidative stress in primary cortical astrocytes using oligonucleotide microarray analysis. *J Biol Chem* 278: 12029–12038

Li H, Li SH, Yu ZX, Shelbourne P, Li XJ (2001) Huntingtin aggregate-associated axonal degeneration is an early pathological event in Huntington's disease mice. *J Neurosci* 21: 8473–8481

Lin MT, Beal MF (2006) Mitochondrial dysfunction and oxidative stress in neurodegenerative diseases. *Nature* 443: 787–795

Linker RA, Lee DH, Ryan S, van Dam AM, Conrad R, Bista P, Zeng W, Hronowsky X, Buko A, Chollate S *et al* (2011) Fumaric acid esters exert neuroprotective effects in neuroinflammation via activation of the Nrf2 antioxidant pathway. *Brain* 134: 678–692

Llorens-Martin M, Jurado J, Hernandez F, Avila J (2014) GSK-3beta, a pivotal kinase in Alzheimer disease. *Front Mol Neurosci* 7: 46

Lopez-Erauskin J, Fourcade S, Galino J, Ruiz M, Schluter A, Naudi A, Jove M, Portero-Otin M, Pamplona R, Ferrer I *et al* (2011) Antioxidants halt axonal degeneration in a mouse model of X-adrenoleukodystrophy. *Ann Neurol* 70: 84–92

Lopez-Erauskin J, Galino J, Ruiz M, Cuezva JM, Fabregat I, Cacabelos D, Boada J, Martinez J, Ferrer I, Pamplona R *et al* (2013) Impaired mitochondrial oxidative phosphorylation in the peroxisomal disease X-linked adrenoleukodystrophy. *Hum Mol Genet* 22: 3296–3305

Lovestone S, Boada M, Dubois B, Hull M, Rinne JO, Huppertz HJ, Calero M, Andres MV, Gomez-Carrillo B, Leon T *et al*, (2015) A phase II trial of tideglusib in Alzheimer's disease. *J Alzheimers Dis* 45: 75–88

Mastroeni R, Bensadoun JC, Charvin D, Aebischer P, Pujol A, Raoul C (2009) Insulin-like growth factor-1 and neurotrophin-3 gene therapy prevents motor decline in an X-linked adrenoleukodystrophy mouse model. *Ann Neurol* 66: 117–122

McMahon M, Itoh K, Yamamoto M, Chanas SA, Henderson CJ, McLellan LI, Wolf CR, Cavin C, Hayes JD (2001) The Cap'n'Collar basic leucine zipper transcription factor Nrf2 (NF-E2 p45-related factor 2) controls both constitutive and inducible expression of intestinal detoxification and glutathione biosynthetic enzymes. *Cancer Res* 61: 3299–3307

Miller WP, Rothman SM, Nascene D, Kivisto T, DeFor TE, Ziegler RS, Eisengart J, Leiser K, Raymond G, Lund TC *et al* (2011) Outcomes after allogeneic hematopoietic cell transplantation for childhood cerebral adrenoleukodystrophy: the largest single-institution cohort report. *Blood* 118: 1971–1978

Mishra HK, Prots I, Havlicek S, Kohl Z, Perez-Branguli F, Boerstler T, Anneser L, Minakaki G, Wend H, Hampl M *et al* (2016) GSK3beta-dependent dysregulation of neurodevelopment in SPG11-patient iPSC model. *Ann Neurol* 79: 826–840

Morales Pantoja IE, Hu CL, Perrone-Bizzozero NI, Zheng J, Bizzozero OA (2016) Nrf2-dysregulation correlates with reduced synthesis and low glutathione levels in experimental autoimmune encephalomyelitis. *J Neurochem* 139: 640–650

Morato L, Galino J, Ruiz M, Calingasan NY, Starkov AA, Dumont M, Naudi A, Martinez JJ, Aubourg P, Portero-Otin M *et al* (2013) Pioglitazone halts axonal degeneration in a mouse model of X-linked adrenoleukodystrophy. *Brain* 136: 2432–2443

Morato L, Ruiz M, Boada J, Calingasan NY, Galino J, Guilera C, Jove M, Naudi A, Ferrer I, Pamplona R *et al* (2015) Activation of sirtuin 1 as therapy for the peroxisomal disease adrenoleukodystrophy. *Cell Death Differ* 22: 1742–1753

Moser HW, Moser AB, Kawamura N, Murphy J, Suzuki K, Schaumburg H, Kishimoto Y (1980) Adrenoleukodystrophy: elevated C26 fatty acid in cultured skin fibroblasts. *Ann Neurol* 7: 542–549

Mosser J, Douar AM, Sarde CO, Kioschis P, Feil R, Moser H, Poustka AM, Mandel JL, Aubourg P (1993) Putative X-linked adrenoleukodystrophy gene shares unexpected homology with ABC transporters. *Nature* 361: 726–730

Muneer Z, Wiesinger C, Voigtlander T, Werner HB, Berger J, Forss-Petter S (2014) Abcd2 is a strong modifier of the metabolic impairments in peritoneal macrophages of ABCD1-deficient mice. *PLoS One* 9: e108655

Neymotin A, Calingasan NY, Wille E, Naseri N, Petri S, Damiano M, Liby KT, Risingsong R, Sporn M, Beal MF *et al* (2011) Neuroprotective effect of Nrf2/ARE activators, CDDO ethylamide and CDDO trifluoroethylamide, in a mouse model of amyotrophic lateral sclerosis. *Free Radic Biol Med* 51: 88–96

von Otter M, Landgren S, Nilsson S, Celojevic D, Bergstrom P, Hakansson A, Nissbrandt H, Drozdzik M, Bialecka M, Kurzawski M *et al* (2010a) Association of Nrf2-encoding NFE2L2 haplotypes with Parkinson's disease. *BMC Med Genet* 11: 36

von Otter M, Landgren S, Nilsson S, Zetterberg M, Celojevic D, Bergstrom P, Minthon L, Bogdanovic N, Andreasen N, Gustafson D *et al* (2010b) Nrf2-encoding NFE2L2 haplotypes influence disease progression but not risk in Alzheimer's disease and age-related cataract. *Mech Ageing Dev* 131: 105–110

Pajares M, Jimenez-Moreno N, Garcia-Yague AJ, Escoll M, de Ceballos ML, Van Leuven F, Rabano A, Yamamoto M, Rojo AI, Cuadrado A (2016) Transcription factor NFE2L2/NRF2 is a regulator of macroautophagy genes. *Autophagy* 12: 1902–1916

Pardo G, Jones DE (2017) The sequence of disease-modifying therapies in relapsing multiple sclerosis: safety and immunologic considerations. *J Neurol* 264: 2351–2374

Parodi B, Rossi S, Morando S, Cordano C, Bragoni A, Motta C, Usai C, Wipke BT, Scannevin RH, Mancardi GL *et al* (2015) Fumarates modulate microglia activation through a novel HCAR2 signaling pathway and rescue synaptic dysregulation in inflamed CNS. *Acta Neuropathol* 130: 279–295

Paupe V, Dassa EP, Goncalves S, Auchere F, Lonn M, Holmgren A, Rustin P (2009) Impaired nuclear Nrf2 translocation undermines the oxidative stress response in Friedreich ataxia. *PLoS One* 4: e4253

Peng H, Li H, Sheehy A, Cullen P, Allaire N, Scannevin RH (2016) Dimethyl fumarate alters microglia phenotype and protects neurons against proinflammatory toxic microenvironments. *J Neuroimmunol* 299: 35–44

Petrillo S, Piemonte F, Pastore A, Tozzi G, Aiello C, Pujol A, Cappa M, Bertini E (2013) Glutathione imbalance in patients with X-linked adrenoleukodystrophy. *Mol Genet Metab* 109: 366–370

Powers JM, Pei Z, Heinzer AK, Deering R, Moser AB, Moser HW, Watkins PA, Smith KD (2005) Adreno-leukodystrophy: oxidative stress of mice and men. *J Neuropathol Exp Neurol* 64: 1067–1079

Pujol A, Hindelang C, Callizot N, Bartsch U, Schachner M, Mandel JL (2002) Late onset neurological phenotype of the X-ALD gene inactivation in mice: a mouse model for adrenomyeloneuropathy. *Hum Mol Genet* 11: 499–505

Pujol A, Ferrer I, Camps C, Metzger E, Hindelang C, Callizot N, Ruiz M, Pampols T, Giros M, Mandel JL (2004) Functional overlap between ABCD1 (ALD) and ABCD2 (ALDR) transporters: a therapeutic target for X-adrenoleukodystrophy. *Hum Mol Genet* 13: 2997–3006

Rada P, Rojo AI, Chowdhry S, McMahon M, Hayes JD, Cuadrado A (2011) SCF/{beta}-TrCP promotes glycogen synthase kinase 3-dependent degradation of the Nrf2 transcription factor in a Keap1-independent manner. *Mol Cell Biol* 31: 1121–1133

Ramsey CP, Glass CA, Montgomery MB, Lindl KA, Ritson GP, Chia LA, Hamilton RL, Chu CT, Jordan-Sciutto KL (2007) Expression of Nrf2 in neurodegenerative diseases. *J Neuropathol Exp Neurol* 66: 75–85

Ring DB, Johnson KW, Henriksen EJ, Nuss JM, Goff D, Kinnick TR, Ma ST, Reeder JW, Samuels I, Slabiak T *et al* (2003) Selective glycogen synthase kinase 3 inhibitors potentiate insulin activation of glucose transport and utilization *in vitro* and *in vivo. Diabetes* 52: 588–595

van Roermund CW, Visser WF, Ijlst L, van Cruchten A, Boek M, Kulik W, Waterham HR, Wanders RJ (2008) The human peroxisomal ABC half transporter ALDP functions as a homodimer and accepts acyl-CoA esters. *FASEB J* 22: 4201–4208

Rojo AI, Sagarra MR, Cuadrado A (2008) GSK-3beta down-regulates the transcription factor Nrf2 after oxidant damage: relevance to exposure of neuronal cells to oxidative stress. *J Neurochem* 105: 192–202

Rojo AI, Innamorato NG, Martin-Moreno AM, De Ceballos ML, Yamamoto M, Cuadrado A (2010) Nrf2 regulates microglial dynamics and neuroinflammation in experimental Parkinson's disease. *Glia* 58: 588–598

Ruiz M, Jove M, Schluter A, Casasnovas C, Villarroya F, Guilera C, Ortega FJ, Naudi A, Pamplona R, Gimeno R *et al* (2015) Altered glycolipid and glycerophospholipid signaling drive inflammatory cascades in adrenomyeloneuropathy. *Hum Mol Genet* 24: 6861–6876

Salazar M, Rojo AI, Velasco D, de Sagarra RM, Cuadrado A (2006) Glycogen synthase kinase-3beta inhibits the xenobiotic and antioxidant cell response by direct phosphorylation and nuclear exclusion of the transcription factor Nrf2. *J Biol Chem* 281: 14841–14851

Sarlette A, Krampfl K, Grothe C, Neuhoff N, Dengler R, Petri S (2008) Nuclear erythroid 2-related factor 2-antioxidative response element signaling pathway in motor cortex and spinal cord in amyotrophic lateral sclerosis. *J Neuropathol Exp Neurol* 67: 1055–1062

Scannevin RH, Chollate S, Jung MY, Shackett M, Patel H, Bista P, Zeng W, Ryan S, Yamamoto M, Lukashev M *et al* (2012) Fumarates promote cytoprotection of central nervous system cells against oxidative stress via the nuclear factor (erythroid-derived 2)-like 2 pathway. *J Pharmacol Exp Ther* 341: 274–284

Schilling S, Goelz S, Linker R, Luehder F, Gold R (2006) Fumaric acid esters are effective in chronic experimental autoimmune encephalomyelitis and suppress macrophage infiltration. *Clin Exp Immunol* 145: 101–107

Schluter A, Espinosa L, Fourcade S, Galino J, Lopez E, Ilieva E, Morato L, Asheuer M, Cook T, McLaren A *et al* (2012) Functional genomic analysis unravels a metabolic-inflammatory interplay in adrenoleukodystrophy. *Hum Mol Genet* 21: 1062–1077

Shan Y, Schoenfeld RA, Hayashi G, Napoli E, Akiyama T, Iodi Carstens M, Carstens EE, Pook MA, Cortopassi GA (2013) Frataxin deficiency leads to defects in expression of antioxidants and Nrf2 expression in dorsal root ganglia of the Friedreich's ataxia YG8R mouse model. *Antioxid Redox Signal* 19: 1481–1493

Shih AY, Imbeault S, Barakauskas V, Erb H, Jiang L, Li P, Murphy TH (2005) Induction of the Nrf2-driven antioxidant response confers neuroprotection during mitochondrial stress *in vivo. J Biol Chem* 280: 22925–22936

da Silva TF, Eira J, Lopes AT, Malheiro AR, Sousa V, Luoma A, Avila RL, Wanders RJ, Just WW, Kirschner DA *et al* (2014) Peripheral nervous system plasmalogens regulate Schwann cell differentiation and myelination. *J Clin Invest* 124: 2560–2570

Stack C, Ho D, Wille E, Calingasan NY, Williams C, Liby K, Sporn M, Dumont M, Beal MF (2011) Triterpenoids CDDO-ethyl amide and CDDO-trifluoroethyl amide improve the behavioral phenotype and brain pathology in a transgenic mouse model of Huntington's disease. *Free Radic Biol Med* 49: 147–158

Tallantyre E, Bo L, Al-Rawashdeh O, Owens T, Polman C, Lowe J, Evangelou N (2010) Clinico-pathological evidence that axonal loss underlies disability in progressive multiple sclerosis. *Mult Scler J* 16: 406–411

Tolosa E, Litvan I, Hoglinger GU, Burn D, Lees A, Andres MV, Gomez-Carrillo B, Leon T, Del Ser T, Investigators T (2014) A phase 2 trial of the GSK-3 inhibitor tideglusib in progressive supranuclear palsy. *Mov Disord* 29: 470–478

Turk BR, Theisen BE, Nemeth CL, Marx JS, Shi X, Rosen M, Jones RO, Moser AB, Watkins PA, Raymond GV *et al* (2017) Antioxidant capacity and superoxide dismutase activity in adrenoleukodystrophy. *JAMA Neurol* 74: 519–524

Vargas CR, Wajner M, Sirtori LR, Goulart L, Chiochetta M, Coelho D, Latini A, Llesuy S, Bello-Klein A, Giugliani R *et al* (2004) Evidence that oxidative stress is increased in patients with X-linked adrenoleukodystrophy. *Biochim Biophys Acta* 1688: 26–32

Wang Q, Li WX, Dai SX, Guo YC, Han FF, Zheng JJ, Li GH, Huang JF (2017) Meta-analysis of Parkinson's disease and alzheimer's disease revealed commonly impaired pathways and dysregulation of NRF2-dependent genes. *J Alzheimers Dis* 56: 1525–1539

Wiesinger C, Kunze M, Regelsberger G, Forss-Petter S, Berger J (2013) Impaired very long-chain acyl-CoA beta-oxidation in human X-linked adrenoleukodystrophy fibroblasts is a direct consequence of ABCD1 transporter dysfunction. *J Biol Chem* 288: 19269–19279